

Identification and Structure–Activity Relationships of Novel Compounds that Potentiate the Activities of Antibiotics in *Escherichia coli*

Keith M. Haynes,[†] Narges Abdali,[‡] Varsha Jhawar,[‡] Helen I. Zgurskaya,[‡] Jerry M. Parks,^{§,||} Adam T. Green,^{§,||} Jerome Baudry,^{§,⊥} Valentin V. Rybenkov,^{‡,||} Jeremy C. Smith,^{§,⊥} and John K. Walker^{*,†,§,||}

[†]Department of Pharmacological & Physiological Science, Saint Louis University School of Medicine, St Louis, Missouri 63104, United States

[‡]Department of Chemistry and Biochemistry, University of Oklahoma, Norman, Oklahoma 73019, United States

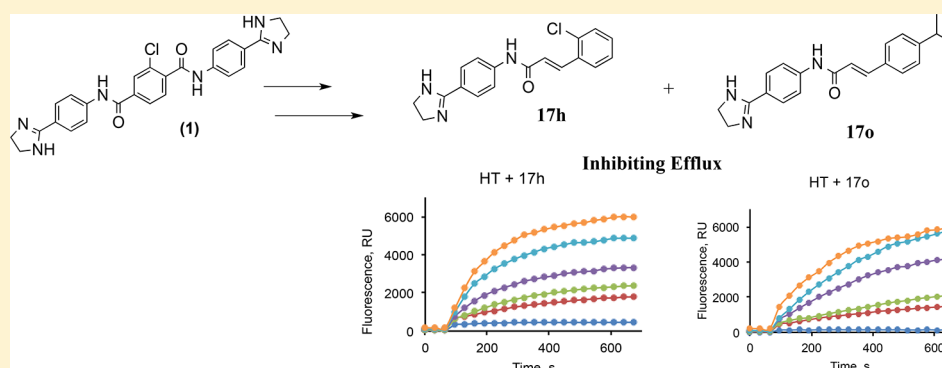
[§]UT/ORNL Center for Molecular Biophysics, Biosciences Division, Oak Ridge National Laboratory, Oak Ridge, Tennessee 37831, United States

^{||}Graduate School of Genome Science and Technology, University of Tennessee, Knoxville, Tennessee 37996, United States

[⊥]Department of Biochemistry and Cellular and Molecular Biology, University of Tennessee, Knoxville, Tennessee 37996, United States

[#]Department of Chemistry, Saint Louis University, St. Louis, Missouri 63104, United States

S Supporting Information



ABSTRACT: In Gram-negative bacteria, efflux pumps are able to prevent effective cellular concentrations from being achieved for a number of antibiotics. Small molecule adjuvants that act as efflux pump inhibitors (EPIs) have the potential to reinvigorate existing antibiotics that are currently ineffective due to efflux mechanisms. Through a combination of rigorous experimental screening and in silico virtual screening, we recently identified novel classes of EPIs that interact with the membrane fusion protein AcrA, a critical component of the AcrAB-TolC efflux pump in *Escherichia coli*. Herein, we present initial optimization efforts and structure–activity relationships around one of those previously described hits, NSC 60339 (1). From these efforts we identified two compounds, SLUPP-225 (17h) and SLUPP-417 (17o), which demonstrate favorable properties as potential EPIs in *E. coli* cells including the ability to penetrate the outer membrane, improved inhibition of efflux relative to 1, and potentiation of the activity of novobiocin and erythromycin.

INTRODUCTION

The number of bacterial pathogens exhibiting resistance to at least one or more classes of antibiotics is on the rise and poses an ever-growing health concern. Resistance to almost all major antibacterial drug classes has been observed in both Gram-negative and Gram-positive species. The situation is particularly acute, with the significant increase in difficult to treat nosocomial infections resulting from Gram-negative bacteria.^{1,2}

In Gram-negative bacteria, one of the primary obstacles to overcome for any antibacterial agent is the synergistic efforts of

the lipopolysaccharide (LPS) rich outer membrane³ (OM) and intracellular efflux pumps. The OM is effective at limiting permeation of drugs into the bacterial cell and efflux pumps located in the cytoplasmic membrane which extrude compounds that do cross the OM back out of the cell before they can reach their potential site of action.^{4,5} Bacterial strains that develop mutations in the OM porins or overexpress efflux

Received: March 24, 2017

Published: June 26, 2017



pumps tend to exhibit greater drug resistance.⁶ As a result, strategies to develop adjuvants that inhibit the action of bacterial efflux pumps (EPI) have the ability to potentiate (i.e., improve antibacterial activity relative to no adjuvant being present) the effectiveness of existing antibacterial agents.^{7–9}

In *Escherichia coli*, the major efflux pump contributing to resistance is the AcrAB-TolC tripartite pump.^{10,11} This class of efflux pumps consists of three separate proteins that assemble to form the active efflux pump complex.^{11,12} The AcrB transporter, which belongs to the resistance nodulation cell division (RND) superfamily of proteins, is responsible for the binding of substrates for efflux. The porin TolC is the channel that spans the OM and allows for passage of substrates from the cell into the extracellular milieu. These two proteins are unable to fully engage on their own but require the membrane fusion protein (MFP) AcrA to bridge the gap between them and form a complete channel that excludes the periplasm.^{11–15} The final composition of the active pump complex is believed to be a 3:6:3 ratio of AcrB:AcrA:TolC.¹⁶ The AcrB substrate-binding protein has been studied extensively as a potential therapeutic target for the development of new EPIs.^{8,17–19} However, until our recent disclosure,²⁰ there were no reports, to the best of our knowledge, of specifically targeting the MFP AcrA as a strategy for the development of EPIs.

We were interested in determining whether assembly of the AcrAB-TolC efflux pump system, and thus its function, could be disrupted via binding of a small molecule to AcrA. Toward that end, the Diversity Set V from the DTP program of the NCI/NIH was screened experimentally and virtual docking was used to identify EPIs that potentially work by targeting AcrA. Experimental screening involved initial evaluation of test compounds in an *E. coli* cell line (WT-pore) engineered to express large pores (~2.4 nm) in the OM.²¹ This approach allowed us to identify compounds that are potential EPIs and might have been overlooked otherwise due to poor OM penetration. Specifically, compounds were tested in the presence of novobiocin at a concentration (16 µg/mL) that is 1/4 of its minimum inhibitory concentration (MIC) in that strain. Test compounds showing MICs ~ 100 µM or better were further evaluated to determine if they were acting as EPIs (vide infra). The other key step involved using surface plasmon resonance^{20,22} (SPR) to determine whether compounds could bind to AcrA. Compounds that potentiated novobiocin and were also found to bind to AcrA in the SPR experiments were prioritized as potential hits.

From the screening efforts, NSC 60339 (**1**)²³ (Figure 1), a polybasic terephthalic acid derivative studied previously^{24,25} as a

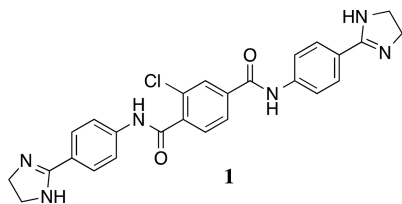


Figure 1. NSC 60339 (**1**).

potential cancer chemotherapeutic agent, stood out as one of the more attractive candidates for medicinal chemistry follow-up. This compound's profile was consistent with an EPI potentially working via binding to AcrA. Testing of **1** in WT-pore cells, in the presence of novobiocin, resulted in an

observed MIC of 25 µM while in the absence of novobiocin it had only weak antibacterial activity (MIC = 200 µM). In SPR experiments with AcrA protein and 50 µM of compound **1**, a strong binding signal was observed. Binding of **1** to AcrA was further established through in vivo proteolysis experiments with AcrA. It was found that the cleavage products of AcrA differed when exposed to **1** compared to control experiments done in the absence of **1**, suggesting **1** binds to AcrA and induces structural changes to AcrA as a result of binding. Furthermore, **1** was shown to dramatically reduce the rate of efflux of a known AcrAB-TolC substrate, bisbenzamide dye H-33342 (HT), in *E. coli* cells.²⁶ Taken together, these findings suggest **1** is an EPI that functions at least in part through binding of AcrA. Lastly, in terms of synthetic feasibility, **1** is a relatively simple terephthalic acid analogue derived from 2-chloroterephthalic acid (**2a**) and aniline **3** (Figure 2). As a result, we envisioned rapid entry into new analogues to explore critical structure–activity relationships (SAR) around this compound.

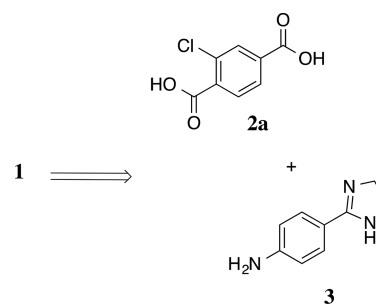


Figure 2. Retrosynthesis of **1**.

Herein we report the synthesis, pharmacological evaluation, and SAR of several new analogues of **1**, some of which demonstrated an equivalent or better profile for potentiation, efflux inhibition, and/or cell penetration. These studies are expected to pave the way for identifying more potent efflux pump inhibitors in the future.

RESULTS AND DISCUSSION

Design. To aid in the selection of novel compounds, we used a previously generated model of AcrA²⁰ (Figure 3A) to

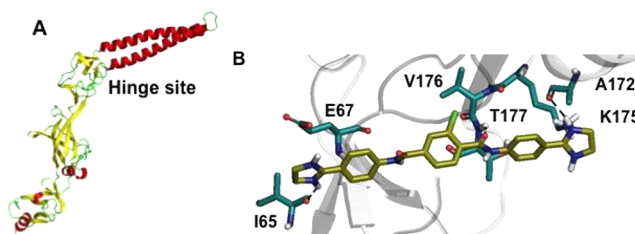


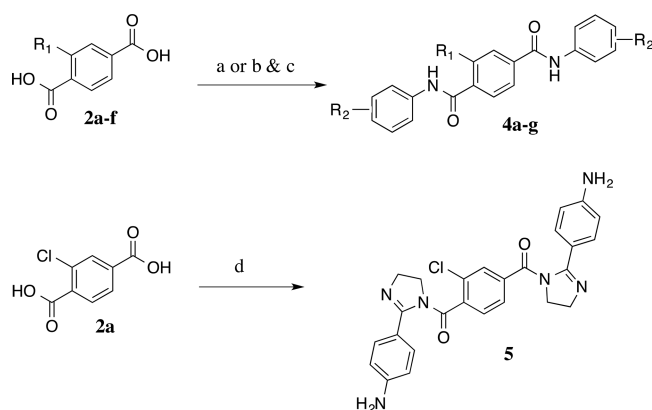
Figure 3. (A) Homology model of AcrA with the hinge site labeled. (B) Highest-ranking docking pose for **1** at the hinge site. Colors: carbon atoms in AcrA and **1** in cyan and gold, respectively; nitrogen in blue; oxygen in red; chlorine in green.

examine relevant possible poses of **1** at the hinge site, which is located at the interface of the α -helical hairpin and the lipoyl domains. The highest ranked pose of **1** was used to suggest possible modifications that may improve binding affinities. The calculated pK_a values for the dihydroimidazole groups are >9, suggesting that **1** is dicationic at pH 7. The two

dihydroimidazolium groups were calculated to interact with the backbone carbonyls of Ile65 and Ala172 (Figure 3B). In addition, the orientation of the chloro group, which interacts with the side chain of Val176, also suggests that modification of this group may alter binding and activity. Our initial set of analogues was designed to test some of these observations. However, we stress that although the binding pose at the hinge site provided guidance for modifying the central and dihydroimidazoline rings, the location of the binding site for **1** has not been determined definitively.

Chemistry. General routes for the preparation of new analogues are outlined in Schemes 1–4. The simple

Scheme 1. General Synthetic Procedures to Prepare the Analogues 4a–g^a



^aReagents and conditions: (a) R_2NH_2 , TBTU, diisopropylethylamine, DMF, rt; (b) 2.0 M $(COCl)_2 \cdot CH_2Cl_2$, cat. DMF, CH_2Cl_2 , 0 °C to rt; (c) evaporate to dryness, dissolve in THF, add Et_3N then add R_2NH_2 , 0 °C; (d) aniline **3**, TBTU, *N,N*-diisopropylethylamine, DMF, rt.

terephthalic acid derivatives **4a–g** were prepared following one of the two straightforward procedures shown in Scheme 1.

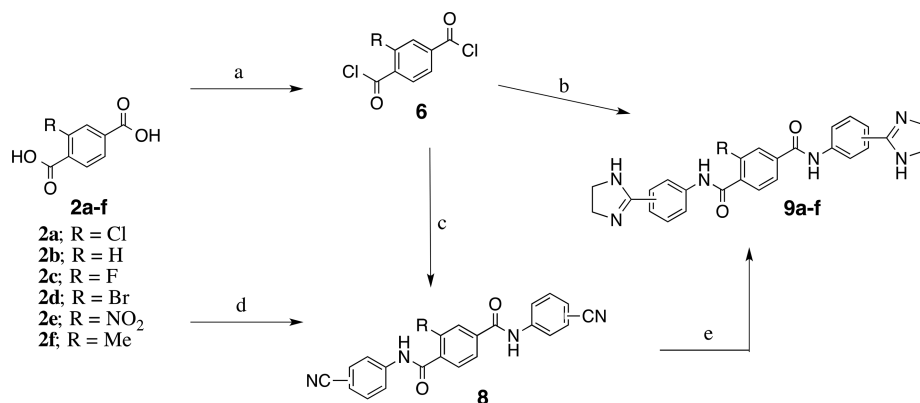
Starting with the desired terephthalic acids **2a** or **2b** and combining with various anilines using a standard peptide coupling approach mediated by *O*-(benzotriazol-1-yl)-*N,N,N',N'*-tetramethyluronium tetrafluoroborate (TBTU) typically led to the desired products in good overall yields. Alternatively, reaction of the appropriate terephthalic acid chlorides with the desired anilines in the presence of an amine base such as *N,N*-diisopropylethylamine also gave the corresponding bis-amide analogues **4a–g** in good yield. However, although perhaps not unexpectedly, neither of these protocols could be extended to coupling reactions involving the dihydroimidazoline-substituted aniline, **3**. For example, when trying to resynthesize **1**, coupling of acid **2a** with aniline **3** using TBTU led exclusively to amide **5**. The same outcome was also realized when using the diacid chloride of **2a** to couple with **3**. None of the desired product from amide formation with the aniline nitrogen was observed (Scheme 1). Interestingly, when amide **5** was profiled in biological testing, it was found to potentiate novobiocin in the WT-pore cells ($MPC_4 = 50 \mu M$).

To prepare analogues **9a–f** from Table 1, as well as to resynthesize **1**, we employed either of the two general procedures shown in Scheme 2. In one procedure, the starting diacids **2a–f** were converted to the corresponding diacid chloride intermediates of type **6** which could subsequently be converted to the nitrile-containing amides **8**. The resulting nitriles, **8**, were then converted to the dihydroimidazoline moiety with ethylenediamine and sodium sulfide following the procedure of Ji et al.²⁷ to give the desired products **9**. The nitriles, **8**, could also be prepared via a standard amide formation protocol using TBTU and either 3-amino (**7a**) or 4-aminobenzonitrile (**7b**). It was also possible to form the desired dihydroimidazoline compounds via a direct coupling of aniline **3** with the diacid chlorides, **6**, in varying yields when the reaction was conducted in glacial acetic acid. The aniline was dissolved in glacial acetic acid first, followed by subsequent

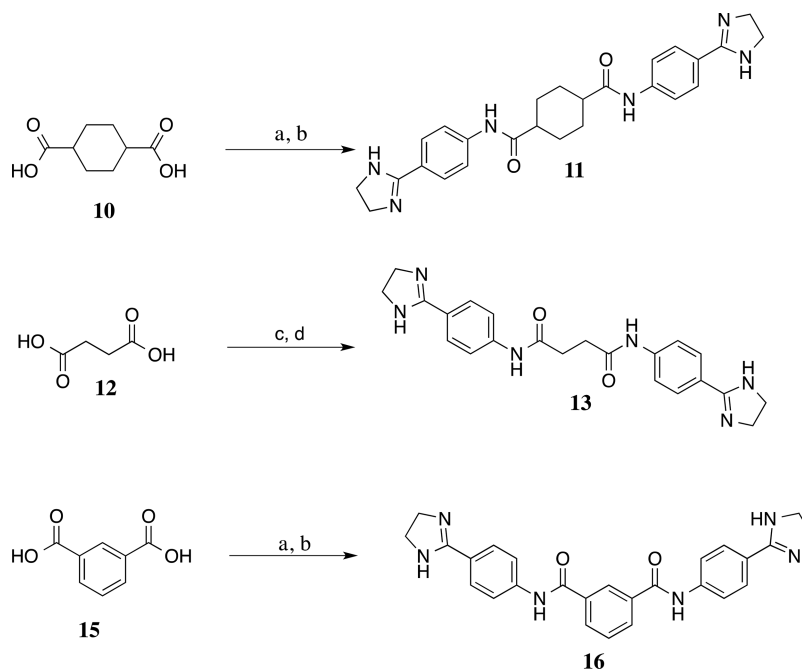
Table 1. Potentiation Values for Related Analogues of 1

#	R ₁	R ₂	MPC ₄ NOV ^a	#	R ₁	R ₂	MPC ₄ NOV ^a
1	-Cl	4,	25 μM	4g	-Cl	4,	>400 μM
4a	-Cl	4, -CN	> 400 μM	9a	-H	3,	50 μM
4b	-Cl	3, -CN	> 400 μM	9b	-H	4,	50 μM
4c	-Cl	4, -CH ₂ OH	> 200 μM	9c	-F	"	100 μM
4d	-H	4, -SO ₃ H	> 100 μM	9d	-Br	"	50 μM
4e	-H	4, -CH ₂ NH ₂	50 μM	9e	-NO ₂	"	25 μM
4f	-Cl	4,	>400 μM	9f	-Me	"	25 μM

^aConcentration of test compound at which novobiocin activity is potentiated 4-fold ($N = 2$).

Scheme 2. General Synthetic Procedures Dihydroimidazoline-Containing Compounds 9a–f^a

^aReagents and conditions: (a) 2.0 M (COCl)₂-CH₂Cl₂, cat. DMF, CH₂Cl₂, 0 °C to rt; (b) aniline 3, HOAc, rt, 1 h; (c) evaporate to dryness, dissolve in THF, add Et₃N then add 3-aminobenzonitrile (7a) or 4-aminobenzonitrile (7b), 0 °C; (d) 7a or 7b, TBTU, diisopropylethyl amine, DMF, rt; (e) H₂NCH₂CH₂NH₂, NaSH, DMAC, 115 °C.

Scheme 3. Synthesis of Analogues 11, 13, and 16^a

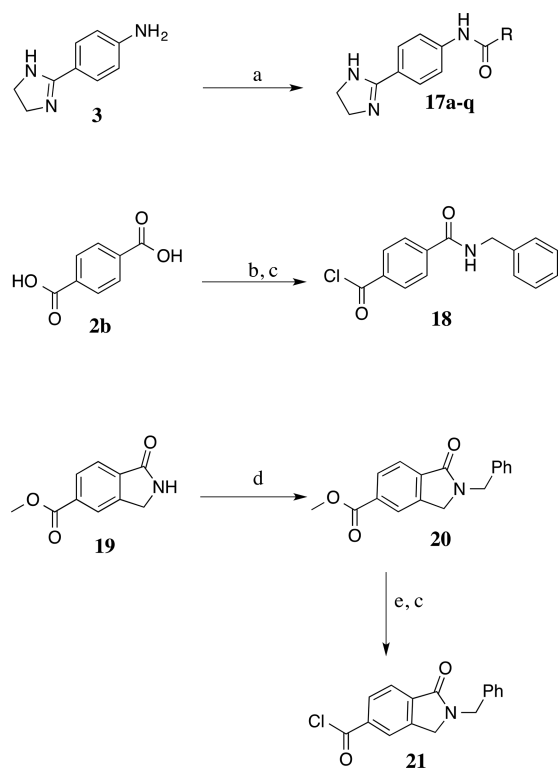
^aReagents and conditions: (a) 7a, TBTU, *N,N*-diisopropylethylamine, DMF, rt; (b) H₂NCH₂CH₂NH₂, NaSH, DMAC, 115 °C; (c) 2.0 M (COCl)₂-CH₂Cl₂, cat. DMF, CH₂Cl₂, 0 °C to rt; (d) aniline 3, HOAc, rt, 1h.

addition of the acid chloride to this mixture.²⁸ In some cases, the solubility of the monoaddition product in glacial acetic acid was poor and the monoaddition product precipitated out of solution before the desired bis-addition product could form. In these cases, the reaction was run in refluxing toluene with a stoichiometric amount of acetic acid.

Analogues 11 and 13, in which the central phenyl has been replaced with a saturated linker, were prepared from *trans*-1,4-cyclohexanedicarboxylic acid (10) and succinic acid (12), respectively, as outlined in Scheme 3. Formation of the nitrile amides followed by conversion of the nitriles to the dihydroimidazoline group led to analogues 11 and 13. The 1,3-diamide analogue, 16, was also prepared in a similar fashion starting from isophthalic acid (15). The known reversed amide compound 14 was prepared as described previously by Dong et al.²⁹

The monoamide derivatives 17a–q shown in Table 3 were prepared as outlined in Scheme 4. In general, aniline 3 was coupled directly to a suitable acid chloride using the glacial acetic acid procedure. The acid chloride, 18, needed to prepare analogue 17c, was made via coupling of terephthalic acid (2b) with benzyl amine (1.3 equiv) mediated by TBTU. This gave rise to a mixture of the desired monobenzylamide and the dibenzyl amide. This mixture was easily separated, and the resulting acid was converted to 18 with oxalyl chloride and catalytic DMF. The isoindoline intermediate 21 was prepared in four total steps from the commercially available ester 19. Exposure of 19 to benzyl bromide in refluxing acetonitrile with cesium carbonate led to efficient introduction of the benzyl group to give 20. Saponification with lithium hydroxide and subsequent acid chloride formation with oxalyl chloride gave the desired acid chloride precursor, 21.

Scheme 4. General Synthetic Procedures for Preparing Analogues 17a–q^a



^aReagents and conditions: (a) RC(O)Cl , **3**, HOAc ; (b) benzyl amine (1.3 equiv), TBTU, *N,N*-diisopropylethylamine, DMF, rt; (c) 2.0 M $(\text{COCl})_2\text{-CH}_2\text{Cl}_2$, cat. DMF, CH_2Cl_2 , 0 °C to rt; (d) BnBr , Cs_2CO_3 , CH_3CN , 75 °C, 2d; (e) LiOH , 9:THF: H_2O .

Cell Assays. To identify compounds that block efflux and potentiate the antibacterial activity of novobiocin, the testing scheme outlined in Figure 4 was followed for all compounds. Compounds were initially evaluated for their ability to prevent bacterial cell growth in combination with novobiocin (16 $\mu\text{g/mL}$, 0.25 MIC) in *E. coli* WT-pore cells. In this way, inhibition of cell growth should be due either to the test compound alone or through working in combination with novobiocin in some manner. In addition, the presence of the large nonspecific pore in the outer membrane of WT-pore cells eliminates the permeability barrier for the compounds and possible non-specific effects on the outer membrane.²¹ Compounds were also evaluated for the ability to inhibit bacterial growth both in the wild-type *E. coli* cells (WT) and in the WT-pore cells in the absence of novobiocin to determine whether they had any intrinsic antibacterial properties. Compounds having an MIC $\leq 100 \mu\text{M}$ in combination with novobiocin were then evaluated in a checkerboard assay to determine the minimum potentiation concentration (MPC) that results in a 4-fold improvement (MPC_4) in the MIC of novobiocin.²⁰ Compounds with an $\text{MPC}_4 \text{ Nov} \leq 50 \mu\text{M}$ were examined for their affinity as substrates for the AcrAB-TolC efflux pump and also their ability to permeate the OM barrier. To accomplish this, compounds were tested in two additional cell-based bacterial growth inhibition assays. One assay tested the compound's ability to inhibit growth in *E. coli* cells engineered to lack the AcrAB-TolC efflux pump (ΔTolC). The other looked at antibacterial activity in *E. coli* cells in which the AcrAB-TolC ($\Delta\text{TolC-pore}$) pump was knocked out and with large pores in the OM. These

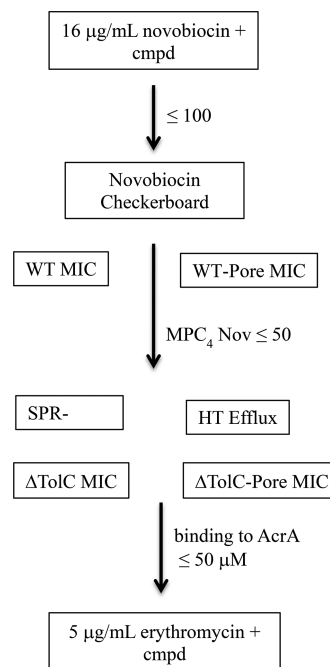


Figure 4. Testing scheme used to identify compounds acting as efflux pump inhibitors.

assays help to define: (i) if potentiation is likely due to blocking the AcrAB-TolC pump or by other mechanisms, (ii) whether the compounds are efflux substrates of the pump, and (iii) how modifications affect the compound's ability to penetrate the OM. Compounds having an $\text{MPC}_4 \text{ Nov} \leq 50 \mu\text{M}$ were also profiled in the SPR and efflux inhibition experiments as described below. Finally, to test the general applicability of this approach, the most promising compounds were tested for their ability to potentiate the macrolide antibiotic erythromycin. As an antibiotic, erythromycin works through a different mechanism of action from novobiocin but it is a substrate for the AcrAB-TolC pump and is therefore only weakly effective against *E. coli*.³⁰ In this way, we can further substantiate the compounds are working generally as EPIs and are not specific just for novobiocin. Similar to experiments with novobiocin, test compounds were administered in the presence of a sublethal dose (5 $\mu\text{g/mL}$, 0.25 MIC) of erythromycin and compounds that potentiated the antibacterial activity of erythromycin were run in the full checkerboard assay format to determine the minimum potentiation concentration.

SPR and HT Assays. In addition to growth inhibition assays, compounds were evaluated for their ability to bind to the purified AcrA protein and to inhibit or slow down the rate of drug efflux in the cell. To determine if new compounds could bind to AcrA, SPR sensorgrams were collected with 50 or 100 μM analyte injected over the purified AcrA protein immobilized onto a CMS sensorchip, using a Biacore instrument. To evaluate the ability of the compound to inhibit drug efflux, the fluorescent HT dye was used. When HT intercalates into membranes or intracellular DNA, it gives a fluorescent signal. HT has also been shown to be a substrate for the AcrAB-TolC efflux pump in *E. coli* that is rapidly effluxed out of the cell.²⁶ As a result, fluorescence from HT accumulation increases very slowly in these cells with active efflux. In the presence of an EPI, however, HT can accumulate in the cell, as indicated by an increase in fluorescence. Therefore, compounds that behave as

EPIs, such as **1**, should accelerate the rate of fluorescence change.

Structure–Activity Relationships. Compound analogues of **1** were prepared to evaluate the roles of the halo substituent (R_1) in the central ring and the dihydroimidazoline moiety in the benzamide groups (R_2) within the hit template (Table 1) using the predicted binding pose at the hinge site as a starting point. The docking calculations suggest that the dihydroimidazoline groups could potentially engage in ionic hydrogen bonding interactions with the backbone carbonyl groups of Ile65, Ala172, or both. To test this hypothesis, we prepared a small set of analogues (**4a–g**) in which the dihydroimidazolines were replaced with groups that are capable of either accepting or donating hydrogen bonds. The cyano analogues, **4a** and **4b**, capable of accepting hydrogen bonds, suffered a significant loss in potentiation. Similarly, the hydroxymethyl compound, **4c**, capable of both accepting and donating hydrogen bonds, also failed to show any significant potentiation activity. The same was also true of the negatively charged sulfonic acid derivative, **4d**. However, the aminomethyl analogue, **4e**, which has estimated pK_a values of ~ 9.0 and 9.6 , showed only a minor reduction in potentiation activity ($MPC_4 = 50 \mu M$) compared to **1** (see Supporting Information, Figure S1 and Table S1, for additional information and docking poses for these compounds). We also prepared the closely related bioisosteres 4-methyl-1,2,4-triazole, **4f**, and imidazole, **4g**, which failed to exhibit any significant potentiation of novobiocin. These findings suggest that a basic nitrogen capable of acting as a hydrogen bond donor is required in this position. When the dihydroimidazoline was shifted from the *para* to the *meta* position, **9a**, we observed only a 2-fold drop ($50 \mu M$) in the MPC_4 value. On the basis of the observed MPC_4 values, replacement of chlorine with a nitro, **9e**, or methyl group, **9f**, had minimal impact on novobiocin potentiation values ($MPC_4 = 25 \mu M$). The bromo, **9d**, and *des*-chloro analogue, **9b**, were also similar to **1**, exhibiting only a 2-fold loss in potentiation. Analogue **9c**, where $R_1 = F$, was the only one to show a significant change in potentiation values with a 4-fold loss being observed. Within the symmetrical starting scaffold, only minor variations in potentiation values were observed for the majority of analogues containing the dihydroimidazoline group. In contrast, significant losses in potentiation were observed when that group was replaced, strongly highlighting that the dihydroimidazoline is critical for activity but the substituent R_1 does not have a dramatic effect on activity. These findings are generally consistent with the model depicting binding in the hinge site where modifications of the dihydroimidazoline ring would be expected to disrupt favorable interactions and reduce the affinity for AcrA.

We also prepared a small number of analogues with changes to the central phenyl ring (Table 2). Preliminary docking experiments suggested that the analogue with a saturated *trans*-cyclohexyl ring, **11**, could bind to AcrA (see Supporting Information, Figure S3). Experimental results, however, showed no potentiation of novobiocin, suggesting that steric hindrance or the lack of aromaticity in the cyclohexyl ring may have a more substantial effect than predicted. Similarly, when the central ring was replaced with a less rigid acyclic core derived from succinic acid, **13**, no potentiation was observed. The reversed amide analogue, **14**, which lacks the chlorine substituent in the central ring, potentiated novobiocin better ($MPC_4 = 12.5 \mu M$) than **1**. Altering the substitution pattern about the central ring, in this case switching from a 1,4-

Table 2. Potentiation of Analogues of **1** with Modifications to the Central Ring

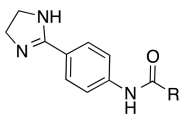
#	Structure	MPC ₄ , NOV ^a (μM)
11		> 400
13		> 400
14		12.5
16		200

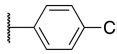
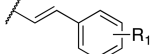
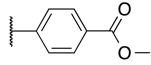
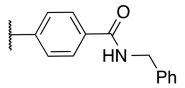
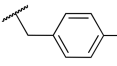
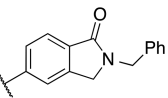
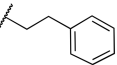
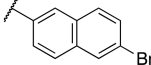
^aConcentration of test compound at which novobiocin activity is potentiated 4-fold ($N = 2$).

disubstituted amide to a 1,3-disubstituted amide, **16**, also led to significant reduction of potentiation activity relative to **1**.

In light of the result with the *meta*-isomer analogue **9a** having similar activity to **1**, we speculated that perhaps only one of the dihydroimidazoline groups is critical for activity. Additionally, docking calculations of **1** identified poses in the AcrA site in which only one of the dihydroimidazoline groups was engaged with the protein (see Supporting Information, Figure S2). With that in mind, we turned our focus to preparing nonsymmetrical analogues derived from addition of aniline **3** to various monoacid chlorides (Scheme 4). We prepared a number of compounds with simple R groups, and several of these are shown in Table 3. Amides derived from simple substituted benzoyl chlorides such as **17a–17c** failed to show any substantial potentiation. The phenylacetamide analogue **17d**, however, did show modest potentiation ($MPC_4 = 100 \mu M$), suggesting that was possible to achieve activity with simpler nonsymmetrical analogues. The dihydroisindoline **17e** and the phenethyl derivative **17f** were also inactive with regard to potentiation. However, the more rigid cinnamoyl derivative, **17g**, did show hints of activity but was somewhat obscured by poor solubility. Replacement of hydrogen with chlorine in the phenyl ring of the cinnamoyl group improved solubility, and both the *ortho*-analogue **17h** and *para*-analogue **17i** showed a marked improvement in potentiation, around $25 \mu M$, while the *meta*-chloro, **17k**, was only slightly worse than these two. Compounds **17h** and **17i** are the first simplified analogues with potentiation at least as good as **1**. Replacement of the 2-chloro with 2-bromo, **17i**, led to a small reduction in potentiation but was still active. A similar result was observed with the 2-trifluoromethyl group, **17j**. As mentioned above, the 4-chloro analogue was active and modifications at this position led to a greater effect on activity. The bromo analogue, **17m**, showed a 2-fold loss in activity relative to **17l**, while the methoxy analogue, **17n**, suffered a 4-fold loss in activity. However, addition of a bulkier alkyl group such as isopropyl, **17o**, or *t*-butyl, **17p**, led to analogues with improved potentiation. With

Table 3. Potentiation for Analogues of 1 Containing Only One Dihydroimidazoline Group



#	R	MPC ₄ , NOV ^a	#	R	MPC ₄ , NOV ^a
17a		200 μM	17g		200 μM
17b		> 400 μM	17h	R ₁ = 2, -Cl	25 μM
17c		> 200 μM	17i	= 2, -Br	50 μM
17d		> 100 μM	17j	= 2, -CF ₃	50 μM
17e		>200 μM	17k	= 3, -Cl	50 μM
17f		> 100 μM	17l	= 4, -Cl	25 μM
			17m	= 4, -Br	100 μM
			17n	= 4, -OMe	100 μM
			17o	= 4, -CH(CH ₃) ₂	50 μM
			17p	= 4, -C(CH ₃) ₃	12.5 μM ^b
			17q		25 μM

^aConcentration of test compound at which novobiocin is potentiated 4-fold ($N = 2$). ^bValue refers to MPC₂, 2-fold potentiation.

the activity shown by the cinnamoyl derivatives, we decided to try a simple naphthyl derivative, **17q**, which would be expected to mimic the conformation of the cinnamoyl derivatives. Indeed, **17q** proved to be active with an MPC₄ value of 25 μM.

Discussion. We identified a number of compounds that potentiated the activity of novobiocin in *E. coli* with values equivalent or better than the original compound, **1**. Several of these were profiled in additional cell-based assays to provide a better understanding of their overall properties (Table 4).

Table 4. SAR Data for Analogues Showing Better Potentiation than 1

compd	MIC (μM) wt ^a	MIC (μM) pore ^b	MIC (μM) ΔTolC ^c	MIC (μM) pore-ΔTolC ^d	AcrA binding ^e	efflux ^f
1	>200	100	25	12.5	+	+
9a	200	100	50	25	+	+
11	50	25	12.5	6.25	—	+
14	50	50	25	12.5	+	—
17h	>200	400	200	100	+	+
17i	>400	>400	200	100	+	+
17l	200	100	50	25	ND ^{g,h}	+
17o	100	50	25	25	++	+
17p	25	25	12.5	12.5	+	+
17q	>400	200	25	12.5	++	+

^aWild-type BW 25113 strain of *E. coli*. ^bEngineered strain of *E. coli* with 2.4 nM pores in the OM. ^c*E. coli* strain with the AcrAB-TolC efflux pump deleted. ^dRepresents a strain of *E. coli* engineered with 2.4 nM pores in the OM and the AcrAB-TolC efflux pump deleted. ^eEvaluation of binding to immobilized AcrA with test compound (25 μM). ^fEvaluation of the rate of cell uptake by HT in the presence of test compound (25 μM). ^gND = not determined. ^hCompound stuck to the SPR control surface ($N = 2$).

Additionally, we assessed their ability to bind to AcrA, inhibit efflux (as measured by HT uptake), and potentiate erythromycin. From this evaluation, compounds that potentiated novobiocin fell into three broad categories: (i) those that do not appear to act primarily through an EPI mechanism, as evidenced by possessing antibacterial activity, weak or no binding to AcrA, and little to no effect on efflux, (ii) those that do appear to act primarily as an EPI, as evidenced by only weak antibacterial activity, binding to AcrA, and a reduced rate of efflux, or (iii) those that possess some characteristics of both (i) and (ii).

One interesting compound that did not fall into the above categories was the cyclohexyl derivative **11**, which did not potentiate novobiocin but did possess antibacterial activity with an MIC = 50 μM in WT cells but decreased only 2-fold in WT-pore cells. This compound showed additional 2-fold reductions in MIC when tested in the ΔTolC and ΔTolC-pore cells, further suggesting it is a weak substrate of the efflux pump and readily penetrates the OM. In agreement with these findings, SPR experiments did not show evidence of binding to AcrA and it only modestly enhanced uptake of HT. The mechanism of action for this antibacterial activity has not been determined. The reversed amide compound, **14**, is an example that falls into the first category described above. It did potentiate novobiocin but is also potent as an antibacterial agent in the WT cells with an MIC = 25 μM. It showed good cell penetration, as its MIC was relatively unaffected in the ΔTolC or ΔTolC-WT-pore cell lines. Unlike **11**, it did bind weakly to AcrA (Figure 5) but did not improve HT uptake in the cells. These two compounds had interesting antibacterial properties with good penetration of the OM but do not appear to be acting as EPIs. The meta-substituted dihydroimidazoline compound, **9a**, a close analogue to **1**, profiled in a similar manner to **1**. It showed only weak

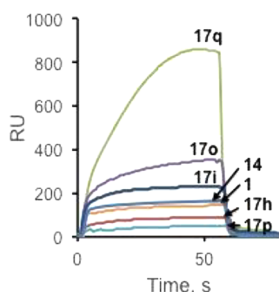


Figure 5. SPR analysis of test compounds (50 μM) binding to immobilized AcrA.

antibacterial activity by itself with an MIC = 200 μM in WT cells. The activity dropped 2-fold in the WT-pore cells and was further reduced to 50 μM in the ΔTolC cells, representing a 4-fold change in activity when the efflux pump was deleted. These results suggest that **9a** acts as an EPI but is also a substrate of the AcrAB-TolC efflux pump. We were unable to detect binding to AcrA because of nonspecific binding of the compound to the chip surface. It did however enhance the rate of HT uptake but at a rate less than that of **1** (see Figure 6).

The *ortho*-halo substituted cinnamoyl derivatives, **17h** and **17i**, were also profiled. Neither compound had appreciable antibacterial activity (MICs > 200 μM) in the WT or WT-pore cells. They both showed a 2-fold decrease in MICs in the ΔTolC cells, suggesting they have some affinity as substrates for the efflux pump. Both were found to bind to AcrA (Figure 5) with greater affinity than **1**, and both yielded a significant enhancement of HT uptake relative to **1** (Figure 6). The analogue with the chloro substituent moved to the 4-position of the cinnamoyl group, **17l**, behaved similarly to that of **17h** but was slightly more potent as an antibiotic, with an MIC = 200 μM in WT cells. When tested in the ΔTolC -pore cells, a 4-

fold reduction in the MIC was observed, similar to what was observed with **17h** and **17i**. Replacing the halo substituent in **17l** with bulkier alkyl groups promoted some significant changes in the properties of these compounds. For instance, the 4-isopropyl analogue **17o** had an MIC = 100 μM in WT cells, while the larger *t*-butyl compound, **17p**, was even more potent with an MIC 4-fold lower at 25 μM . The target responsible for the greater antibacterial activity of **17p** remains unclear at present. The MICs of these compounds in the ΔTolC cells were only 2-fold lower than in the WT cells, suggesting both **17o** and **17p** are less prone to efflux by the TolC efflux pump (Table 5) relative to the other analogues

Table 5. Analysis of SAR Data Comparing Ratios between Different Cell Types

compd	OM ^a	eff ^b	HT ^c	NOV pot ^d	Ery pot ^e
1	4	8	3.2	16	8
9a	2	4	1.7	4	4
17h	1	4	9.7	32	8
17i	1	8	11.6	32	32
17l	2	4	2.5	8	4
17o	2	2	6.3	8	8
17p	1	2	2.6	2	2
17q	4	16	16	16	16

^aEvaluation of OM permeability, ratio of WT MIC/WT-pore MIC.

^bEvaluation of compound susceptibility to efflux, ratio of WT-pore MIC/pore- ΔTolC MIC. ^cRate HT uptake in the presence of 25 μM test compound/HT uptake alone. ^dWT-pore/WT-pore + novobiocin (16 $\mu\text{g/mL}$) MIC. ^eWT-pore MIC/WT-pore + erythromycin (5 $\mu\text{g/mL}$) MIC.

tested. The isopropyl analogue **17o** showed one of the strongest binding signals to AcrA we observed in addition to showing a strong enhancement of HT uptake. The *t*-butyl

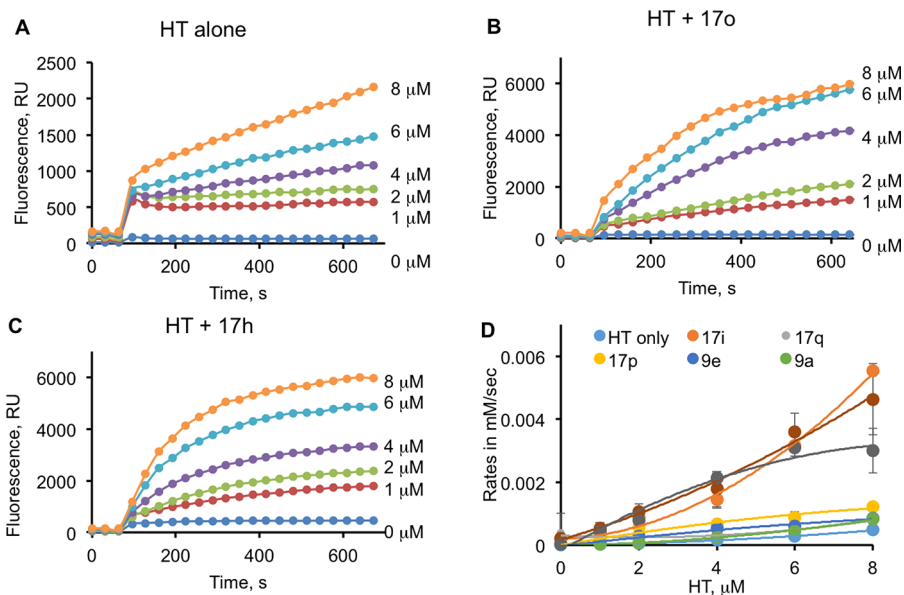


Figure 6. Kinetic analyses of intracellular uptake of HT alone and in the presence of EPIs. (A) Real-time changes in HT fluorescence as a function of time. Exponentially grown and induced WT-pore cells were collected, washed, and resuspended in a buffered glucose solution. HT alone was added to cells (arrows) at increasing concentrations, and fluorescence was monitored over a period of time. (B,C) The same as in (A), but HT was premixed either with 12.5 μM of compound **17o** or 12.5 μM compound **17h** (*E. coli*). Data were collected as above with various analogues, and the kinetic curves were fitted into a two-exponential model to extract the initial rates of uptake. The rates are plotted as a function of HT concentration in the solution ($N = 4$, error bars are SD).

analogue **17p** also showed binding to AcrA with a 2.6-fold rate enhancement of the HT uptake rate. Finally, we evaluated the naphthyl compound, **17q**, which showed relatively little activity in the WT cells with only a slight improvement in the WT-pore cells. However, in the Δ TolC-pore cells, it had an MIC = 12.5 μ M, representing a 16-fold increase in antibacterial activity when the pump was removed. This compound is clearly a strong substrate for the AcrAB-TolC efflux pump. It also displayed strong binding to AcrA but with only a slight enhancement in rate (1.6-fold improvement) for HT uptake in cells.

Because of the cationic nature of these compounds, the possibility exists that they might disrupt the proton motive force that drives the AcrAB-TolC efflux pump. To address this point, we evaluated **1** and the analogues **17h** and **17o** for their effects on the transmembrane potential in *E. coli* cells (Figure 7A). From the data, it appears that our compounds had no

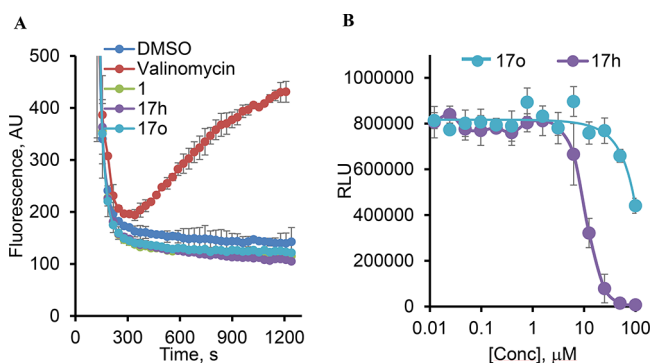


Figure 7. (A) Effect of EPIs on the transmembrane potential in live *E. coli* cells. Valinomycin, but not EPIs or DMSO, affected the transmembrane potential of WT-0ore cells, as seen from the time-dependent increase in DiSc3(5) fluorescence. (B) Evaluation of HEK293 cell viability in the presence of test compounds **17h** and **17o** (IC_{50} values = 10.5 and <100 μ M, respectively, $N = 4$).

effect on the membrane potential, providing further evidence they work primarily through binding of AcrA and disrupting the efflux pump assembly. Additionally, because many of these compounds contain a cinnamoyl moiety, which has the potential to act as a Michael acceptor, we performed a basic cytotoxicity assay in HEK293 cells with **17h** and **17o** (Figure 7B). The cytotoxicity of the two compounds differed significantly, with IC_{50} s of 10.5 and >100 μ M, respectively. From this data, it does not appear that cytotoxicity contributes to the potentiation activity of **17o** but we cannot rule out that it does not make a minor contribution to the potentiation seen with **17h**. Overall, it does not appear that the cinnamoyl group poses a major liability with these compounds. The difference in observed cytotoxicity IC_{50} s is likely due to the nature of the substitution in the cinnamoyl ring.

From a chemical properties standpoint, these new analogues of **1** are characterized primarily by a reduction in molecular weight (MW) (~120–150 Da), increased rigidity, and an increased amphiphilic moment. The latter two properties, along with low globularity and the presence of an unhindered basic nitrogen, were recently shown to be favorable for antibiotic accumulation in Gram-negative bacteria.³¹ These compounds fall nicely within the favorable property range for crossing the OM of Gram-negative bacteria (see Supporting Information, Table 2S), which is consistent with our own experimental data.

Additionally, with the reduced MW, we have the flexibility to optimize these molecules for binding to AcrA, antibacterial targets, or introduce additional modifications to the cinnamoyl group to mitigate potential risk while remaining in the optimal chemical space.

From the data collected a few general SAR trends can be observed. Substitution about the phenyl ring in the cinnamoyl moiety greatly influences the profile of these compounds. Analogues with substituents in the 2-position (i.e., **17h** and **17i**) tend to have lower antibacterial activity, some susceptibility to be substrates for efflux, and also inhibit efflux to a greater extent than other analogues. These compounds also are very effective at crossing the OM as measured by the ratio of activities in WT vs WT-pore cells (Table 5). Conversely, substitution in the 4-position (i.e., **17l**, **17o**, and **17p**) led to compounds with greater antibacterial activity and less susceptibility to efflux but also were less effective at inhibiting efflux. Like the other cinnamoyl derivatives, these compounds are also effective at crossing the OM. The more rigid naphthyl compound **17q** is interesting because it shows the greatest affinity for AcrA in the SPR experiments, but it is also the most susceptible to efflux by the AcrAB-TolC efflux pump. That it does not show greater potentiation is likely attributed to its greater susceptibility to efflux. It is also one of the few analogues that are unable to cross the OM readily, with a ratio similar to the original lead, **1**. Finally, all of the compounds are able to potentiate the activity of a second antibiotic, erythromycin (see Table 5). Erythromycin is a macrolide antibiotic that is ineffective against *E. coli* because it is a substrate for AcrAB-TolC. Erythromycin potentiation values for these compounds are consistent with those of novobiocin, further suggesting these compounds are working as EPIs. Taken together, our findings suggest that there are subtle factors that influence whether these compounds act as EPIs, are substrates for efflux, or bind to an antibacterial target. In many cases, the compounds exhibit more than one of these characteristics. Of the compounds tested, analogues **17h** and **17o** appear to be the most promising for future development. Both readily cross the OM, bind to AcrA, and inhibit efflux in *E. coli* by potentiating the activity of two separate antibiotics.

CONCLUSION

In this report, we have identified several novel potentiators of novobiocin and erythromycin in *E. coli*. These compounds were designed starting from the recently identified inhibitor **1** with the objective of inhibiting the AcrAB-TolC efflux pump by interacting with the MFP constituent AcrA of the AcrAB-TolC efflux pump. In many cases, the new compounds were shown to bind AcrA and also to inhibit efflux to some extent in assays measuring the uptake of the fluorescent probe HT into cells. Two compounds of particular interest are **17h** and **17o**, both of which show good potentiation of novobiocin and erythromycin, bind to AcrA, and inhibit efflux at a rate significantly higher than the original hit. They differ slightly in that the chloro-substituted analogue **17h** has minimal antibacterial activity on its own while **17o** has a good MIC in wild-type cells. Another important aspect of this class of compounds is that they show the potential to cross the outer membrane of Gram-negative bacteria. In summary, we have identified compounds with diverse characteristics that inhibit efflux and potentiate the antibacterial properties of novobiocin and erythromycin in *E. coli*. Some of these compounds are significantly more potent than our original lead, **1**.

■ EXPERIMENTAL SECTION

General Methods. Compounds **1** and **4d** (NSC 55156) were obtained from the National Cancer Institute. Novobiocin, erythromycin, and Hoechst 33342 were obtained from Sigma-Aldrich Chemie GMBH (Steinham, Germany). All reagents and solvents for the synthesis of analogues **4a–g**, **5**, **9a–f**, and **17a–g** were purchased from Sigma-Aldrich Chemie GMBH (Steinham, Germany), Alfa Aesar GMBH & Co KG (Karlsruhe, Germany), Acros Organics (Geel, Belgium), TCI America (Portland, United States) or Enamine Ltd. (Monmouth, United States) and used as is without further purification. The purities of the final compounds were characterized by high-performance liquid chromatography (HPLC) using a gradient elution program (Ascentis Express Peptide C18 column, acetonitrile/water 5/95 → 95/5, 5 min, 0.05% trifluoroacetic acid) and UV detection (254 nm). The purities of all compounds final compounds were 95% or greater. ¹H NMR and ¹³C NMR were obtained on a Bruker 400 MHz instrument and all chemical shifts are referenced to residual solvent peaks.

PAINS. All of the biologically tested compounds were evaluated for structural attributes consistent with classification as pan-assay interference compounds (PAINS).³² The results for each compound were negative.

2-Chloro-*N*¹,*N*⁴-bis(4-(4,5-dihydro-1*H*-imidazol-2-yl)phenyl)-terephthalamide (1**).** 2-Chloroterephthalic acid (50 mg, 0.25 mmol) was converted to the corresponding acid chloride via treatment with 2.0 M oxalyl chloride solution (0.312 mL, 0.625 mmol) in dichloromethane. A catalytic quantity of dimethylformamide was added, and the reaction was complete in 4 h on an ice bath. 2-Chloroterephthaloyl dichloride was dried to a yellow solid and dissolved in 1.5 mL of anhydrous toluene. In a second vial, sodium acetate (150 mg, 1.8 mmol) was dissolved in 2.5 mL of glacial acetic acid. To this vial, 4-(4,5-dihydro-1*H*-imidazol-2-yl)aniline (88 mg, 0.55 mmol) was added and the mixture sonicated until a homogeneous solution was achieved. The acetic acid solution was added dropwise to the acid chloride, purged with argon, and allowed to react overnight at room temperature. Product precipitated and was collected by filtration. Crude product was dissolved in a minimal amount of water before being made basic with 4.0 M sodium hydroxide solution. Solution was then heated at 50 °C until product had completely precipitated as free-base. Precipitate was collected and triturated with methanol to yield product as a white solid (18 mg, 15% yield). ¹H NMR (400 MHz, DMSO-*d*₆) δ 10.84 (s, 1H), 10.61 (s, 1H), 8.17 (s, 1H), 8.05 (d, *J* = 8.0 Hz, 1H), 7.82 (m, 9H), 3.63 (s, 8H). ¹³C NMR (400 MHz, DMSO-*d*₆) δ 164.59, 163.70, 139.21, 137.00, 130.15, 129.15, 128.78, 128.34, 128.29, 128.23, 128.17, 126.81, 119.79, 119.05, 48.21. HRMS: *m/z* calcd for C₂₆H₂₃ClN₆O₂ [M + H]⁺ 487.1651; found [M + H]⁺ 487.1691, [M + 2H]⁺ 244.0863.

2-Chloro-*N*¹,*N*⁴-bis(4-cyanophenyl)terephthalamide (4a**).** A solution of 2-chloroterephthalic acid (50 mg, 0.25 mmol) in 2.0 mL of dichloromethane was cooled to 0 °C using an ice bath. To this solution was added sequentially a catalytic amount (~1–2 drops) of DMF followed by a 2.0 M solution of oxalyl chloride (1.68 mL, 3.3 mmol) in dichloromethane. The resulting mixture was stirred overnight, allowing the temperature to gradually warm to rt. The resulting mixture was concentrated down to dryness on a rotoevaporator and then dried under vacuum for 2 h. The resulting solid was then dissolved in 3.0 mL of THF and cooled to 0 °C in an ice bath. To this mixture was added triethyl amine (0.087 mL, 1.2 mmol), and the reaction was stirred for 5 min. To this mixture was added 4-aminobenzonitrile (74 mg, 0.62 mmol) as a solution in 1.0 mL of THF. The resulting mixture was stirred for 1 h at 0 °C and then allowed to warm to rt and stir for 2 h. The reaction was quenched with saturated solution of sodium bicarbonate, which led to the formation of a white precipitate. The precipitate was isolated by filtration and rinsed several times with deionized water. The resulting solid was collected and dried under vacuum to give a white solid (69 mg, 69%). ¹H NMR (400 MHz, DMSO-*d*₆) δ 10.96 (s, 2H), 8.18 (d, *J* = 1.6 Hz, 1H), 8.06 (dd, *J* = 8.0, 1.6 Hz, 1H), 7.99 (d, *J* = 8.8 Hz, 2H), 7.91 (d, *J*

= 8.8 Hz, 2H), 7.824 (m, 5H). HRMS: *m/z* calcd for C₂₂H₁₃ClN₄O₂ [M + H]⁺ 401.0807; found [M + H]⁺ 401.0780.

2-Chloro-*N*¹,*N*⁴-bis(4-cyanophenyl)terephthalamide (4b**).** Compound **4b** was prepared according to the procedure outlined above for example **4a** using 3-aminobenzonitrile (white solid, yield 85%). ¹H NMR (400 MHz, DMSO-*d*₆) δ 10.72 (s, 2H), 8.28 (m, 2H), 8.13 (s, 4H), 8.07 (m, 2H), 7.61 (m, 4H). HRMS: *m/z* calcd for C₂₂H₁₄N₄O₂ [M + H]⁺ 367.1197; found [M + H]⁺ 367.1199.

2-Chloro-*N*¹,*N*⁴-bis(4-(hydroxymethyl)phenyl)terephthalamide (4c**).** To a 25 mL round-bottom flask with stir bar, 4-aminobenzyl alcohol (0.500 g, 4.05 mmol) and imidazole (0.303 g, 4.46 mmol) were added. Dichloromethane (10.0 mL) was added followed by the addition of *tert*-butyldimethylsilyl chloride (0.610 g, 4.05 mmol). The reaction was allowed to stir overnight at room temperature and stopped with addition of ethyl acetate, which induces precipitation of byproducts that can be filtered off before extraction with water. The organic layer was dried with sodium sulfate and concentrated down to a thick oil before being purified on a 25 g silica flash column with 40% ethyl acetate in hexane. 4-(((*tert*-Butyldimethylsilyl)oxy)methyl)-aniline obtained as colorless oil after drying on high vacuum overnight (0.944 g, 98% yield). ¹H NMR (400 MHz, CDCl₃) δ 8.98 (s, 1H), 8.83 (s, 1H), 7.71 (t, *J* = 7.2 Hz, 4H), 7.63 (d, *J* = 2.0 Hz, 1H), 7.52 (dd, *J* = 8.0, 1.6 Hz, 1H), 7.42 (d, *J* = 8.0 Hz, 1H), 7.32 (dd, *J* = 8.4, 4.8 Hz, 4H), 4.73 (d, *J* = 2.8 Hz, 4H), 0.95 (d, *J* = 0.8 Hz, 18H), 0.109 (d, *J* = 1.2 Hz, 12H).

To a reaction vial with magnetic stir bar and Teflon cap, 2-chloroterephthalic acid (100 mg, 0.50 mmol) and TBTU (320 mg, 1.00 mmol) were added and the vial was purged with argon. Then 5.0 mL DMF was added through the cap followed by diisopropylethylamine (0.44 mL, 2.50 mmol). The reaction was allowed to stir for 15 min at room temperature before the addition of 4-(((*tert*-butyldimethylsilyl)oxy)methyl)aniline (296 mg, 1.25 mmol). The reaction was run overnight before being quenched with water and extracted into ethyl acetate. The organic layer was treated with sodium sulfate and dried to give an oil. The product was run through a 25 g silica flash column with 2% methanol in dichloromethane and dried to a white solid (256 mg, 80% yield). Cleavage of the TBDMS group was achieved by dissolving the compound in THF (5.0 mL), followed by addition of 0.1 M tetrabutylammonium fluoride (0.98 mL) and stirring overnight. The reaction mixture was dried to a solid and run through a 24 g silica flash column with 2% methanol in dichloromethane. The product was dried to a white solid (37 mg, 22% yield). ¹H NMR (400 MHz, DMSO-*d*₆) δ 10.58 (s, 1H), 10.40 (s, 1H), 8.14 (d, *J* = 1.6 Hz, 1H), 8.03 (dd, *J* = 8.0, 1.6 Hz, 1H), 7.74 (m, 3H), 7.67 (d, *J* = 8.8 Hz, 2H), 7.31 (dd, *J* = 8.8, 4 Hz, 4H) 5.15 (dt, *J* = 5.6, 1.6 Hz, 2H), 4.48 (dd, *J* = 5.6, 3.2 Hz, 4H). ¹³C NMR (400 MHz, DMSO-*d*₆) δ 164.22, 163.26, 139.38, 138.27, 138.21, 137.33, 137.08, 130.11, 129.01, 128.59, 126.96, 126.81, 126.61, 120.27, 119.41, 62.59, 62.56. HRMS: *m/z* calcd for C₂₂H₁₉ClN₂O₄ [M + H]⁺ 411.1113; found [M + H]⁺ 411.1090.

***N*¹,*N*⁴-Bis(4-(aminomethyl)phenyl)terephthalamide (**4e**).** To a reaction vial with magnetic stir bar and Teflon cap, terephthaloyl chloride (40 mg, 0.20 mmol) was added along with 2.0 mL of anhydrous dichloromethane. 4-((*N*-Boc)aminomethyl)aniline (93 mg, 0.42 mmol) was added along with triethylamine (0.06 mL, 0.42 mmol). The vial was purged with argon and allowed to react overnight at room temperature. Methanol was added to the reaction mixture, and it was filtered to collect the Boc-protected product as a white solid. The protecting group was removed with the addition of TFA and stirred for 4 h before drying to a solid. The crude product was sonicated in 4 M NaOH and filtered to collect the product as a white solid (21 mg, 28% yield). ¹H NMR (400 MHz, DMSO-*d*₆) δ 10.50 (s, 2H), 8.11 (s, 8H), 7.83 (d, *J* = 8.4 Hz, 4H), 7.45 (d, *J* = 8.4 Hz, 4H), 4.02 (s, 4H). ¹³C NMR (400 MHz, DMSO-*d*₆) δ 164.88, 139.19, 137.32, 129.46, 129.36, 127.85, 120.53, 42.00. HRMS: *m/z* calcd for C₂₂H₂₂N₄O₂ [M + H]⁺ 375.1823; found [M + H]⁺ 375.1822, [M + 2H]⁺ 171.0680.

2-Chloro-*N*¹,*N*⁴-bis(4-(4-methyl-4*H*-1,2,4-triazol-3-yl)phenyl)-terephthalamide (4f**).** Compound **4f** was prepared from 2-chloroterephthalic acid and 4-(4-methyl-4*H*-1,2,4-triazol-3-yl)aniline

as described above for the synthesis of compound **4a** (white solid, yield 57%). ¹H NMR (400 MHz, DMSO-*d*₆) δ 10.89 (s, 1H), 10.66 (s, 1H), 8.56 (s, 2H), 8.20 (d, *J* = 0.8 Hz, 1H), 8.08 (dd, *J* = 7.6, 1.6 Hz, 1H), 7.99 (d, *J* = 8.8 Hz, 2H), 7.91 (d, *J* = 8.8 Hz, 2H), 7.83 (d, *J* = 7.6 Hz, 1H), 7.78 (m, 4H), 3.76 (d, *J* = 3.6 Hz, 6H). HRMS: *m/z* calcd for C₂₆H₂₁ClN₈O₂ [M + H]⁺ 513.1556; found [M + H]⁺ 513.1557, [M + 2H]⁺ 257.0821.

N¹,N⁴-Bis(4-(1H-imidazol-2-yl)phenyl)-2-chloroterephthalamide (4g). Compound **4g** was prepared from 2-chloroterephthalic acid and 4-(1H-imidazol-2-yl)aniline as described above for the synthesis of compound **4a** (white solid, yield 24%). ¹H NMR (400 MHz, DMSO-*d*₆) δ 12.48 (s, 2H), 10.75 (s, 1H), 10.54 (s, 1H), 8.18 (d, *J* = 1.6 Hz, 1H), 8.06 (dd, *J* = 7.6, 1.6 Hz, 1H), 7.93 (m, 4H), 7.88 (d, *J* = 9.2 Hz, 2H), 7.80 (m, 3H), 7.13 (s, 4H). ¹³C NMR (400 MHz, DMSO-*d*₆) δ 164.38, 163.45, 139.32, 138.64, 138.58, 137.09, 130.18, 129.14, 128.70, 126.72, 126.41, 125.45, 125.30, 120.50, 119.72.

(2-Chloro-1,4-phenylene)bis((2-(4-aminophenyl)-4,5-dihydro-1H-imidazol-1-yl)methanone) (5). 2-Chloroterephthalic acid (102 mg, 0.51 mmol) was added to a reaction vial with a stir bar. TBTU was added (327 mg, 1.02 mmol) before the addition of 10 mL of anhydrous DMF. Diisopropylethylamine (0.45 mL, 2.55 mmol) was added and the reaction stirred for 10 min before the addition of 4-(4,5-dihydro-1H-imidazol-2-yl)aniline (**3**) (210 mg, 1.29 mmol). The vial was purged with argon and allowed to react overnight at room temperature before extracting the product into dichloromethane from water. The organic layer was dried with sodium sulfate and dried to a solid on a rotavap. It was then purified on an ISCO 12 g silica column (4% methanol in DCM). The product was obtained as a yellow solid (51 mg, 21% yield). ¹H NMR (400 MHz, DMSO-*d*₆) δ 7.43 (s, 3H), 7.15 (s, 4H), 6.39 (s, 4H), 5.47 (m, 4H), 3.81 (s, 8H).

N¹,N⁴-Bis(3-(4,5-dihydro-1H-imidazol-2-yl)phenyl)-terephthalamide (9a). Compound **9a** was prepared from bis-nitrile intermediate **N¹,N⁴-bis(3-(4,5-dihydro-1H-imidazol-2-yl)phenyl)-terephthalamide, 4b**, as described below for the preparation of compound **9b** (white solid; yield 30%). ¹H NMR (400 MHz, DMSO-*d*₆) δ 10.85 (s, 2H), 10.60 (s, 4H), 8.54 (m, 2H), 8.17 (s, 4H), 7.98 (m, 2H), 7.68 (m, 4H), 4.03 (s, 8H). ¹³C NMR (400 MHz, DMSO-*d*₆) δ 165.32, 165.07, 139.65, 137.01, 129.73, 128.01, 126.58, 124.07, 122.76, 120.36, 44.43. HRMS: *m/z* calcd for C₂₆H₂₄N₆O₂ [M + H]⁺ 453.2041; found [M + H]⁺ 453.2043, [M + 2H]⁺ 227.1057.

N¹,N⁴-Bis(4-(4,5-dihydro-1H-imidazol-2-yl)phenyl)-terephthalamide Dihydrochloride (9b). To a reaction vial with magnetic stir bar and Teflon cap, terephthaloyl dichloride (70 mg, 0.34 mmol) and 4-aminobenzonitrile (100 mg, 0.86 mmol) were added and vial was purged with argon. Then 3.0 mL THF was added along with trimethylamine (0.12 mL, 0.86 mmol). The reaction was allowed to stir at room temperature overnight. The reaction was quenched with the addition of saturated sodium bicarbonate solution and filtered to collect crude product, which was then purified with trituration in methanol to collect **N¹,N⁴-bis(4-(cyanophenyl)terephthalamide** intermediate as a white solid (107 mg, 86% yield). ¹H NMR (400 MHz, DMSO-*d*₆) δ 10.92 (s, 2H), 8.21 (s, 4H), 8.02 (d, *J* = 9.2 Hz, 4H), 7.85 (d, *J* = 8.8 Hz, 4H).

N¹,N⁴-Bis(4-cyanophenyl)terephthalamide (40 mg, 0.11 mmol) was added to a 2 dram vial with stir bar. Ethylenediamine (0.768 mL, 11.5 mmol) was added along with 1.0 mL of dimethylacetamide before the addition of sodium hydrosulfide hydrate (88 mg, 1.57 mmol). The solution was capped and carefully heated to 115 °C. The reaction was set on a timer and allowed to react 12 h with constant stirring. Once cooled, the reaction was quenched with water to precipitate product and filtered to collect product as the free base, which was not soluble in dimethyl sulfoxide. It was then converted to the HCl salt by adding 8 equiv HCl as a 4.0 M solution in dioxane and heating at 90 °C for 1 h. The product was collected as a white solid (19 mg, 39% yield) and converted to the triflate salt with trifluoroacetic acid (1 equiv). ¹H NMR (400 MHz, DMSO-*d*₆) δ 10.95 (s, 2H), 10.47 (s, 4H), 8.17 (s, 4H), 8.10 (d, *J* = 9.2 Hz, 4H), 8.01 (d, *J* = 9.2 Hz, 4H), 4.00 (s, 8H). ¹³C NMR (400 MHz, DMSO-*d*₆) δ 165.47, 164.42, 144.55, 137.24, 129.53, 128.07, 120.05, 116.80, 44.32. HRMS: *m/z* calcd for

C₂₆H₂₄N₆O₂ [M + H]⁺ 453.2041; found [M + H]⁺ 453.2038, [M + 2H]⁺ 227.1061.

N¹,N⁴-Bis(4-(4,5-dihydro-1H-imidazol-2-yl)phenyl)-2-fluoroterephthalamide (9c). Compound **9c** was prepared from 2-fluoroterephthalic acid and 4-(4,5-dihydro-1H-imidazol-2-yl)aniline as outlined above for compound **1**. White solid, converted to TFA salt, yield 18%. ¹H NMR (400 MHz, DMSO-*d*₆) δ 11.15 (s, 1H), 10.99 (s, 1H), 10.52 (s, 1H), 8.11 (d, *J* = 9.2 Hz, 2H), 8.02 (m, 8H), 7.91 (t, *J* = 8.0 Hz, 1H), 4.01 (s, 8H). HRMS: *m/z* calcd for C₂₆H₂₃FN₆O₂ [M + H]⁺ 471.1947; found [M + H]⁺ 471.1945, [M + 2H]⁺ 236.1010.

N¹,N⁴-Bis(4-(4,5-dihydro-1H-imidazol-2-yl)phenyl)-2-bromoterephthalamide (9d). Compound **9d** was prepared from 2-bromoterephthalic acid and 4-(4,5-dihydro-1H-imidazol-2-yl)aniline as outlined above for compound **1** (tan solid, yield 17%). ¹H NMR (400 MHz, DMSO-*d*₆) δ 10.79 (s, 1H), 10.58 (s, 1H), 8.31 (d, *J* = 1.6 Hz, 1H), 8.08 (dd, *J* = 4.8, 2.0 Hz, 1H), 7.84 (d, *J* = 4.4 Hz, 4H), 7.81 (s, 2H), 7.76 (m, 3H), 3.61 (s, 8H). ¹³C NMR (400 MHz, DMSO-*d*₆) δ 165.43, 163.49, 163.22, 163.17, 141.45, 140.69, 140.58, 136.98, 131.73, 128.94, 127.94, 127.77, 127.23, 125.68, 125.18, 119.71, 119.05, 118.95, 49.36. HRMS: *m/z* calcd for C₂₆H₂₃BrN₆O₂ [M + H]⁺ 531.1146; found [M + H]⁺ 531.1120.

N¹,N⁴-Bis(4-(4,5-dihydro-1H-imidazol-2-yl)phenyl)-2-nitroterephthalamide (9e). Compound **9e** was prepared from 2-nitroterephthalic acid and 4-(4,5-dihydro-1H-imidazol-2-yl)aniline as outlined above for compound **1** (white solid, yield 9%). ¹H NMR (400 MHz, DMSO-*d*₆) δ 10.95 (s, 1H), 10.77 (s, 1H), 8.73 (d, *J* = 1.6 Hz, 1H), 8.45 (dd, *J* = 4.8, 1.6 Hz, 1H), 8.00 (d, *J* = 8.0 Hz, 1H), 7.84 (m, 6H), 7.72 (d, *J* = 8.8 Hz, 2H), 3.61 (s, 8H). ¹³C NMR (400 MHz, DMSO-*d*₆) δ 163.72, 163.22, 163.18, 162.88, 146.28, 140.47, 140.46, 136.81, 134.80, 133.26, 129.81, 128.01, 127.83, 126.04, 125.92, 123.58, 119.83, 119.01, 49.52. HRMS: *m/z* calcd for C₂₆H₂₃N₇O₄ [M + H]⁺ 498.1892; found [M + H]⁺ 498.1896, [M + 2H]⁺ 249.5984.

N¹,N⁴-Bis(4-(4,5-dihydro-1H-imidazol-2-yl)phenyl)-2-methylterephthalamide (9f). Compound **9f** was prepared from 2-methylterephthalic acid and 4-(4,5-dihydro-1H-imidazol-2-yl)aniline as outlined above for compound **9b** (white solid, yield 44%). ¹H NMR (400 MHz, DMSO-*d*₆) δ 11.00 (s, 1H), 10.88 (s, 1H), 8.10 (d, *J* = 9.2, 2H), 8.02 (m, 7H), 7.96 (d, *J* = 8.4, 1H), 7.69 (d, *J* = 8.0 Hz, 1H), 3.99 (s, 8H), 2.49 (s, 3H). ¹³C NMR (400 MHz, DMSO-*d*₆) δ 167.37, 165.05, 140.92, 140.88, 139.73, 135.61, 135.57, 129.79, 127.82, 127.71, 127.39, 125.14, 119.59, 118.98, 49.35, 19.36. HRMS: *m/z* calcd for C₂₇H₂₆N₆O₂ [M + H]⁺ 467.2197; found [M + H]⁺ 467.2183.

(1*r*,4*r*)-N¹,N⁴-Bis(4-(4,5-dihydro-1H-imidazol-2-yl)phenyl)-cyclohexane-1,4-dicarboxamide (11). Compound **11** was prepared from the bis-nitrile (**1*r*,4*r*)-N¹,N⁴-bis(4-cyanophenyl)cyclohexane-1,4-dicarboxamide, following the procedure described above for compound **9b** (white solid, yield 23%). ¹H NMR (400 MHz, DMSO-*d*₆) δ 10.52 (s, 2H), 7.93 (d, *J* = 9.6 Hz, 4H), 7.87 (d, *J* = 8.8 Hz, 4H), 3.98 (s, 8H), 3.04 (s, 2H), 1.96 (d, *J* = 6.8 Hz, 4H), 1.49 (t, *J* = 10.0 Hz, 4H). ¹³C NMR (400 MHz, DMSO-*d*₆) δ 174.93, 164.38, 144.96, 129.66, 118.73, 115.88, 44.29, 44.14, 28.07. HRMS: *m/z* calcd for C₂₆H₃₀N₆O₂ [M + H]⁺ 459.2510; found [M + H]⁺ 459.2512, [M + 2H]⁺ 230.1294.**

N¹,N⁴-Bis(4-(4,5-dihydro-1H-imidazol-2-yl)phenyl)succinamide (13). Succinic acid (35 mg, 0.3 mmol) was converted to the corresponding acid chloride via treatment with 2.0 M oxalyl chloride solution in dichloromethane. A catalytic quantity of DMF was added, and the reaction was complete in 4 h on an ice bath. The solvent was removed, leaving succinyl chloride as a yellow solid. 4-(4,5-Dihydro-1H-imidazol-2-yl)aniline (97 mg, 0.6 mmol) was dissolved in 1.5 mL of glacial acetic acid before being added to the acid chloride. The solution was sonicated to mix before being allowed to react overnight at room temperature. The solvent was removed, and crude product was purified on a 50 g C18 reversed-phase column (acetonitrile/water). White solid, 2 TFA salt, yield 9%. ¹H NMR (400 MHz, DMSO-*d*₆) δ 10.57 (s, 2H), 10.34 (s, 4H), 7.89 (d, *J* = 9.2 Hz, 4H), 7.82 (d, *J* = 8.8 Hz, 4H), 3.98 (s, 8H), 2.75 (s, 4H). ¹³C NMR (400 MHz, DMSO-*d*₆) δ 171.37, 164.37, 144.76, 129.69, 118.56, 115.83, 44.26, 30.95. HRMS: *m/z* calcd for C₂₂H₂₄N₆O₂ [M + H]⁺ 405.2041; found [M + H]⁺ 405.2041, [M + 2H]⁺ 203.1056.

*N*¹,*N*³-Bis(4-(4,5-dihydro-1*H*-imidazol-2-yl)phenyl)-isophthalamide (**16**). Compound **16** was prepared from the bis-nitrile, *N*¹,*N*³-bis(4-cyanophenyl)isophthalamide, following the procedure described above for compound **9a**. White solid, 2 HCl salt, yield 45%. ¹H NMR (400 MHz, DMSO-*d*₆) δ 11.20 (s, 2H), 10.44 (s, 4H), 8.84 (s, 1H), 8.21 (m, 6H), 8.01 (d, *J* = 8.8 Hz, 4H), 7.76 (t, *J* = 7.6 Hz, 1H), 4.00 (s, 8H). ¹³C NMR (400 MHz, DMSO-*d*₆) δ 165.48, 164.29, 144.79, 134.14, 131.66, 129.49, 119.81, 116.59, 44.22. HRMS: *m/z* calcd for C₂₆H₂₄N₆O₂ [M + H]⁺ 453.2041; found [M + H]⁺ 453.2037, [M + 2H]⁺ 227.1056.

4-Chloro-*N*-(4-(4,5-dihydro-1*H*-imidazol-2-yl)phenyl)benzamide (**17a**). 4-Chlorobenzoic acid (47 mg, 0.3 mmol) was converted to the corresponding acid chloride via treatment with 2.0 M oxalyl chloride solution (0.18 mL, 0.36 mmol) in dichloromethane. A catalytic quantity of DMF was added, and the reaction was complete in 4 h on an ice bath. The solvent was removed, leaving 4-chlorobenzoyl chloride as a yellow solid. 4-(4,5-Dihydro-1*H*-imidazol-2-yl)aniline (48 mg, 0.3 mmol) was dissolved in 1.5 mL of glacial acetic acid before being added to the acid chloride. The solution was sonicated to mix before being allowed to react overnight at room temperature. The solvent was removed, and crude product was purified on a 50 g C18 reversed-phase column (acetonitrile/water). The product was obtained as a TFA salt (45 mg, 36% yield). ¹H NMR (400 MHz, DMSO-*d*₆) δ 10.76 (s, 1H), 10.36 (s, 2H), 8.04 (d, *J* = 8.8 Hz, 2H), 8.00 (d, *J* = 8.4 Hz, 2H), 7.94 (d, *J* = 9.2 Hz, 2H), 7.66 (d, *J* = 8.8 Hz, 2H), 4.00 (s, 4H). ¹³C NMR (400 MHz, DMSO-*d*₆) δ 165.11, 164.39, 144.57, 136.95, 129.81, 129.47, 128.59, 119.92, 116.63, 44.28. HRMS: *m/z* calcd for C₁₆H₁₄ClN₃O [M + H]⁺ 300.0905; found [M + H]⁺ 300.0904.

Methyl 4-((4-(4,5-Dihydro-1*H*-imidazol-2-yl)phenyl)carbamoyl)-benzoate (**17b**). Compound **17b** was prepared from 4-(methoxycarbonyl)benzoic acid and 4-(4,5-dihydro-1*H*-imidazol-2-yl)aniline (**3**) following the procedure described above for compound **17a** (tan solid, yield 32%). ¹H NMR (400 MHz, DMSO-*d*₆) δ 10.63 (s, 1H), 8.10 (dd, *J* = 12.8, 8.8 Hz, 4H), 7.85 (dd, *J* = 16.5, 9.2 Hz, 4H), 3.90 (s, 3H), 3.65 (s, 4H). ¹³C NMR (400 MHz, DMSO-*d*₆) δ 165.65, 165.02, 163.47, 141.62, 138.75, 132.23, 129.23, 128.19, 128.15, 119.70, 52.47. HRMS: *m/z* calcd for C₁₈H₁₇N₃O₃ [M + H]⁺ 324.1350; found [M + H]⁺ 324.1352.

*N*¹-Benzyl-*N*⁴-(4-(4,5-dihydro-1*H*-imidazol-2-yl)phenyl)-terephthalamide (**17c**). Compound **17c** was prepared from acid chloride **18**, described below, and 4-(4,5-dihydro-1*H*-imidazol-2-yl)aniline (**3**) following the procedure described above for compound **17a** (white solid, yield 25%). ¹H NMR (400 MHz, DMSO-*d*₆) δ 10.53 (s, 1H), 9.24 (s, 1H), 8.05 (s, 4H), 7.84 (s, 4H), 7.31 (m, 5H), 4.52 (s, 2H), 3.60 (s, 4H). ¹³C NMR (400 MHz, DMSO-*d*₆) δ 165.48, 165.04, 163.15, 140.66, 139.50, 139.48, 137.05, 136.95, 128.33, 127.78, 127.61, 127.32, 127.27, 126.82, 126.06, 119.59, 42.72. HRMS: *m/z* calcd for C₂₄H₂₂N₄O₂ [M + H]⁺ 399.1823; found [M + H]⁺ 399.1828.

2-(4-Chlorophenyl)-*N*-(4-(4,5-dihydro-1*H*-imidazol-2-yl)phenyl)-acetamide (**17d**). Compound **17d** was prepared from 2-(4-chlorophenyl)acetic acid and 4-(4,5-dihydro-1*H*-imidazol-2-yl)aniline (**3**) following the procedure described above for compound **17a**. Tan solid, TFA salt, yield 11%. ¹H NMR (400 MHz, DMSO-*d*₆) δ 10.70 (s, 1H), 10.32 (s, 2H), 7.88 (d, *J* = 9.2 Hz, 2H), 7.83 (d, *J* = 8.8 Hz, 2H), 7.40 (d, *J* = 8.4 Hz, 2H), 7.35 (d, *J* = 8.8 Hz, 2H), 3.98 (s, 4H), 3.73 (s, 2H). ¹³C NMR (400 MHz, DMSO-*d*₆) δ 169.77, 164.34, 144.61, 134.41, 131.45, 131.17, 129.68, 128.28, 118.81, 116.18, 44.27, 42.41. HRMS: *m/z* calcd for C₁₇H₁₆ClN₃O [M + H]⁺ 314.1062; found [M + H]⁺ 314.1059.

2-Benzyl-*N*-(4-(4,5-dihydro-1*H*-imidazol-2-yl)phenyl)-1-oxoisoin-doline-5-carboxamide (**17e**). Ester **20** (75 mg, 0.48 mmol) was dissolved in 5 mL of a 9:1 mixture of THF–H₂O and stirred vigorously. To this mixture was added LiOH (25 mg, 1 mmol), and the reaction was stirred at rt overnight. The reaction was judged complete, and the solvent was removed to near dryness by passing a gentle stream of air over the vial. The resulting residue was neutralized to ~pH 5–6 with 1 N HCl, and the product was extracted with dichloromethane (4×). The organics, were combined, dried, and

concentrated in vacuo. The resulting acid was converted to the acid chloride without further purification.

The acid (55 mg, 0.23 mmol) was added to a vial fitted with a Teflon screwcap and slurried in 1.5 mL of dichloromethane. The reaction was then cooled to 0 °C, and a catalytic amount of DMF (0.01 mL) was added followed by addition of 2.0 M solution of oxalyl chloride (0.125 mL, 0.5 mmol) in dichloromethane. The resulting solution was stirred at 0 °C for 10 min then allowed to warm to rt and stirred for 1 h to give a dark-yellow homogeneous solution. The solvent was then removed under vacuum to give a yellow-brown residue and further dried under vacuum for 2 h. In a separate vial, 4-(4,5-dihydro-1*H*-imidazol-2-yl)aniline (**3**) (37 mg, 0.23 mmol) was dissolved in 1 mL of glacial acetic acid. The resulting homogeneous mixture was stirred for 5 min at rt and then added all at once to the acid chloride residue from above. A thick yellow precipitate formed, and the reaction was allowed to stir overnight. The resulting reaction mixture was filtered through a fritted funnel with washing from diethyl ether and then dried. The solid is then slurried in water, and a saturated sodium bicarbonate solution was added until the pH ~ 10. The solution was then filtered and washed sequentially with water and diethyl ether and further dried under vacuum to give a tan solid (15 mg, 16%). This was converted to the TFA salt as described above. ¹H NMR (400 MHz, DMSO-*d*₆) δ 10.90 (s, 1H), 10.41 (s, 2H), 8.13 (s, 1H), 8.09 (d, *J* = 7.6 Hz, 1H), 8.05 (d, *J* = 9.2 Hz, 2H), 7.95 (d, *J* = 8.8 Hz, 2H), 7.91 (d, *J* = 8.0 Hz, 1H), 7.37 (m, 2H), 7.30 (m, 3H), 4.78 (s, 2H), 4.48 (s, 2H), 4.00 (s, 4H). ¹³C NMR (400 MHz, DMSO-*d*₆) δ 166.53, 165.88, 164.42, 141.92, 137.28, 137.13, 129.53, 128.75, 127.75, 127.68, 127.45, 123.32, 123.05, 119.95, 116.72, 49.40, 45.53, 44.30. HRMS: *m/z* calcd for C₂₅H₂₂N₄O₂ [M + H]⁺ 411.1823; found [M + H]⁺ 411.1801.

N-(4-(4,5-Dihydro-1*H*-imidazol-2-yl)phenyl)-3-phenylpropanamide (**17f**). Compound **17f** was prepared from 3-phenylpropanoic acid and 4-(4,5-dihydro-1*H*-imidazol-2-yl)aniline (**3**) following the procedure described above for compound **17a**. White solid, TFA salt, yield 28%. ¹H NMR (400 MHz, DMSO-*d*₆) δ 10.43 (s, 1H), 10.31 (s, 2H), 7.87 (d, *J* = 9.2 Hz, 2H), 7.81 (d, *J* = 8.8 Hz, 2H), 7.27 (m, 4H), 7.10 (t, *J* = 6.8 Hz, 1H), 3.98 (s, 4H), 2.92 (t, *J* = 7.6 Hz, 2H), 2.70 (t, *J* = 8.0 Hz, 2H). ¹³C NMR (400 MHz, DMSO-*d*₆) δ 171.46, 164.38, 144.71, 140.96, 129.68, 128.37, 128.27, 126.04, 118.67, 115.93, 44.27, 38.00, 30.53. HRMS: *m/z* calcd for C₁₈H₁₉N₃O [M + H]⁺ 294.1608; found [M + H]⁺ 294.1607.

N-(4-(4,5-Dihydro-1*H*-imidazol-2-yl)phenyl)cinnamamide (**17g**). Compound **17g** was prepared from cinnamic acid and 4-(4,5-dihydro-1*H*-imidazol-2-yl)aniline (**3**) following the procedure described above for compound **17a**. Tan solid, TFA salt, yield 20%. ¹H NMR (400 MHz, DMSO-*d*₆) δ 13.48 (s, 1H), 10.90 (s, 1H), 8.81 (d, *J* = 2.4 Hz, 1H), 8.71 (s, broad, 2H), 8.67 (s, 1H), 8.36 (d, *J* = 2.0 Hz, 1H), 8.09 (m, 4H), 7.86 (d, *J* = 8.8 Hz, 1H), 7.78 (dd, *J* = 8.8, 2.0 Hz, 1H), 6.61 (s, 1H), 2.60 (s, 3H). ¹³C NMR (400 MHz, DMSO-*d*₆) δ 164.41, 164.31, 144.82, 141.54, 134.46, 130.18, 129.73, 129.11, 127.96, 121.56, 118.96, 116.19, 44.29. HRMS: *m/z* calcd for C₁₈H₁₇N₃O [M + H]⁺ 292.1452; found [M + H]⁺ 292.1449.

(*E*)-3-(2-Chlorophenyl)-*N*-(4-(4,5-dihydro-1*H*-imidazol-2-yl)phenyl)acrylamide (**17h**). Compound **17h** was prepared from (*E*)-3-(2-chlorophenyl)acrylic acid and 4-(4,5-dihydro-1*H*-imidazol-2-yl)aniline (**3**) following the procedure described above for compound **17a** (white solid, yield 16%). ¹H NMR (400 MHz, DMSO-*d*₆) δ 10.55 (s, 1H), 7.90 (d, *J* = 15.6 Hz, 1H), 7.79 (m, 5H), 7.57 (m, 1H), 7.45 (m, 2H), 6.92 (d, 15.6 Hz, 1H), 3.62 (s, 4H). ¹³C NMR (400 MHz, DMSO-*d*₆) δ 163.27, 163.23, 141.05, 135.71, 133.50, 132.43, 131.34, 130.11, 128.01, 127.90, 127.74, 125.16, 124.96, 118.62, 49.09. HRMS: *m/z* calcd for C₁₈H₁₆ClN₃O [M + H]⁺ 326.1062; found [M + H]⁺ 326.1060.

(*E*)-3-(2-Bromophenyl)-*N*-(4-(4,5-dihydro-1*H*-imidazol-2-yl)phenyl)acrylamide (**17i**). Compound **17i** was prepared from (*E*)-3-(2-bromophenyl)acrylic acid and 4-(4,5-dihydro-1*H*-imidazol-2-yl)aniline (**3**) following the procedure described above for compound **17a**. White solid, TFA salt, yield 34%. ¹H NMR (400 MHz, DMSO-*d*₆) δ 10.85 (s, 1H), 10.36 (s, 2H), 7.92 (m, 5H), 7.78 (dd, *J* = 7.6, 1.6 Hz, 1H), 7.75 (dd, *J* = 8.0, 1.2 Hz, 1H), 7.51 (t, *J* = 7.2 Hz, 1H), 7.38

(dt, $J = 8.0, 1.6$ Hz, 1H), 6.89 (d, $J = 15.6$ Hz, 1H), 4.00 (s, 4H). ^{13}C NMR (400 MHz, DMSO- d_6) δ 164.39, 163.74, 144.61, 139.21, 133.97, 133.42, 131.82, 129.78, 128.52, 127.90, 124.74, 124.59, 119.11, 116.44, 44.32. HRMS: m/z calcd for $\text{C}_{18}\text{H}_{16}\text{BrN}_3\text{O}$ $[\text{M} + \text{H}]^+$ 370.0557; found $[\text{M} + \text{H}]^+$ 370.0559.

(*E*)-*N*-(4-(4,5-Dihydro-1*H*-imidazol-2-yl)phenyl)-3-(2-(trifluoromethyl)phenyl)acrylamide (**17j**). Compound **17j** was prepared from (*E*)-3-(2-(trifluoromethyl)phenyl)acrylic acid and 4-(4,5-dihydro-1*H*-imidazol-2-yl)aniline (**3**) following the procedure described above for compound **17a**. White solid, TFA salt, yield 16%. ^1H NMR (400 MHz, DMSO- d_6) δ 10.93 (s, 1H), 10.39 (s, 2H), 7.87 (m, 8H), 7.66 (t, $J = 7.6$ Hz, 1H), 6.95 (d, $J = 15.2$ Hz, 1H), 4.00 (s, 4H). ^{13}C NMR (400 MHz, DMSO- d_6) δ 164.40, 163.45, 144.44, 135.98, 133.26, 132.86, 130.19, 129.74, 127.97, 127.19, 126.90, 126.12, 119.16, 116.53, 44.3;

(*E*)-3-(3-Chlorophenyl)-*N*-(4-(4,5-dihydro-1*H*-imidazol-2-yl)phenyl)acrylamide (**17k**). Compound **17k** was prepared from (*E*)-3-(3-chlorophenyl) acrylic acid and 4-(4,5-dihydro-1*H*-imidazol-2-yl)aniline (**3**) following the procedure described above for compound **17a**. White solid, TFA salt, yield 16%. ^1H NMR (400 MHz, DMSO- d_6) δ 10.74 (s, 1H), 10.34 (s, 2H), 7.93 (s, 4H), 7.74 (s, 1H), 7.64 (m, 2H), 7.50 (m, 2H), 6.91 (d, $J = 15.6$ Hz, 1H), 4.00 (s, 4H). ^{13}C NMR (400 MHz, DMSO- d_6) δ 164.39, 163.97, 144.65, 139.81, 136.76, 133.77, 130.89, 129.72, 127.62, 126.33, 123.32, 118.98, 116.29, 44.28. HRMS: m/z calcd for $\text{C}_{18}\text{H}_{16}\text{ClN}_3\text{O}$ $[\text{M} + \text{H}]^+$ 326.1062; found $[\text{M} + \text{H}]^+$ 326.1036.

(*E*)-3-(4-Chlorophenyl)-*N*-(4-(4,5-dihydro-1*H*-imidazol-2-yl)phenyl)acrylamide (**17l**). Compound **17l** was prepared from (*E*)-3-(4-chlorophenyl) acrylic acid and 4-(4,5-dihydro-1*H*-imidazol-2-yl)aniline (**3**) following the procedure described above for compound **17a**. White solid, TFA salt, yield 35%. ^1H NMR (400 MHz, DMSO- d_6) δ 10.74 (s, 1H), 10.33 (s, 2H), 7.93 (s, 2H), 7.66 (m, 3H), 7.54 (d, $J = 8.4$ Hz, 2H), 6.86 (d, 16.4 Hz, 1H), 3.99 (s, 4H). ^{13}C NMR (400 MHz, DMSO- d_6) δ 164.38, 164.09, 144.71, 140.09, 134.58, 133.42, 129.71, 129.61, 129.12, 122.38, 118.97, 116.23, 44.31. HRMS: m/z calcd for $\text{C}_{18}\text{H}_{16}\text{ClN}_3\text{O}$ $[\text{M} + \text{H}]^+$ 326.1062; found $[\text{M} + \text{H}]^+$ 326.1053.

(*E*)-3-(4-Bromophenyl)-*N*-(4-(4,5-dihydro-1*H*-imidazol-2-yl)phenyl)acrylamide (**17m**). Compound **17m** was prepared from (*E*)-3-(4-bromophenyl) acrylic acid and 4-(4,5-dihydro-1*H*-imidazol-2-yl)aniline (**3**) following the procedure described above for compound **17a**. Yellow solid, TFA salt, yield 22%. ^1H NMR (400 MHz, DMSO- d_6) δ 10.44 (s, 1H), 10.31 (s, 2H), 7.87 (d, $J = 9.2$ Hz, 2H), 7.80 (d, 9.2 Hz, 2H), 7.47 (d, $J = 8.4$ Hz, 2H), 7.21 (d, $J = 8.0$ Hz, 2H), 3.98 (s, 4H), 2.90 (t, $J = 7.6$ Hz, 2H), 2.70 (t, $J = 7.6$ Hz, 2H). ^{13}C NMR (400 MHz, DMSO- d_6) δ 171.22, 164.34, 144.64, 140.44, 131.19, 130.62, 129.68, 119.07, 118.67, 115.94, 44.26, 37.64, 29.81. HRMS: m/z calcd for $\text{C}_{18}\text{H}_{16}\text{BrN}_3\text{O}$ $[\text{M} + \text{H}]^+$ 372.0713; found $[\text{M} + \text{H}]^+$ 372.0706.

(*E*)-*N*-(4-(4,5-Dihydro-1*H*-imidazol-2-yl)phenyl)-3-(4-methoxyphenyl)acrylamide (**17n**). Compound **17n** was prepared from (*E*)-3-(4-methoxyphenyl) acrylic acid and 4-(4,5-dihydro-1*H*-imidazol-2-yl)aniline (**3**) following the procedure described above for compound **17a** (tan solid, yield 6%). ^1H NMR (400 MHz, DMSO- d_6) δ 10.63 (s, 1H), 10.32 (s, 2H), 7.92 (d, $J = 2.8$ Hz, 4H), 7.61 (m, 3H), 7.03 (d, $J = 8.4$ Hz, 2H), 6.71 (d, $J = 15.6$ Hz, 1H), 3.99 (s, 4H), 3.81 (s, 3H).

(*E*)-*N*-(4-(4,5-Dihydro-1*H*-imidazol-2-yl)phenyl)-3-(4-isopropylphenyl)acrylamide (**17o**). Compound **17o** was prepared from (*E*)-3-(4-isopropylphenyl) acrylic acid and 4-(4,5-dihydro-1*H*-imidazol-2-yl)aniline (**3**) following the procedure described above for compound **17a**. White solid, TFA salt, yield 8%. ^1H NMR (400 MHz, DMSO- d_6) δ 10.70 (s, 1H), 10.33 (s, 2H), 7.93 (d, $J = 2.8$ Hz, 4H), 7.61 (m, 3H), 7.34 (d, $J = 8.8$ Hz, 2H), 6.81 (d, $J = 15.6$ Hz, 1H), 3.99 (s, 4H), 2.93 (m, 1H), 1.22 (d, $J = 6.8$ Hz, 6H). ^{13}C NMR (400 MHz, DMSO- d_6) δ 164.46, 164.40, 150.91, 144.89, 141.55, 132.12, 129.74, 128.09, 127.09, 120.53, 118.93, 116.11, 44.29, 33.40, 23.68. HRMS: m/z calcd for $\text{C}_{21}\text{H}_{23}\text{N}_3\text{O}$ $[\text{M} + \text{H}]^+$ 334.1921; found $[\text{M} + \text{H}]^+$ 334.1906.

(*E*)-3-(4-(*tert*-Butyl)phenyl)-*N*-(4-(4,5-dihydro-1*H*-imidazol-2-yl)phenyl)acrylamide (**17p**). Compound **17p** was prepared from (*E*)-3-

(4-*tert*-butylphenyl) acrylic acid and 4-(4,5-dihydro-1*H*-imidazol-2-yl)aniline (**3**) following the procedure described above for compound **17a**. White solid, TFA salt, yield 7%. ^1H NMR (400 MHz, DMSO- d_6) δ 10.70 (s, 1H), 10.33 (s, 2H), 7.93 (d, $J = 2.8$ Hz, 4H), 7.61 (m, 3H), 7.49 (d, $J = 8.8$ Hz, 2H), 6.82 (d, $J = 15.6$ Hz, 1H), 3.99 (s, 4H), 1.30 (s, 9H). ^{13}C NMR (400 MHz, DMSO- d_6) δ 164.43, 164.37, 153.04, 144.87, 141.36, 131.71, 129.70, 127.78, 125.87, 120.63, 118.89, 116.07, 44.26, 34.63, 30.92. HRMS: m/z calcd for $\text{C}_{22}\text{H}_{25}\text{N}_3\text{O}$ $[\text{M} + \text{H}]^+$ 348.2078; found $[\text{M} + \text{H}]^+$ 348.2049.

6-Bromo-*N*-(4-(4,5-dihydro-1*H*-imidazol-2-yl)phenyl)-2-naphthamide (**17q**). 6-Bromo-2-naphthoic acid (63 mg, 0.25 mmol) was converted to the corresponding acid chloride via treatment with 2.0 M oxalyl chloride solution (0.15 mL, 0.3 mmol) in dichloromethane. A catalytic quantity of DMF was added, and the reaction was complete in 4 h on an ice bath. The solvent was removed, leaving 6-bromo-2-naphthoyl chloride as a yellow solid. 4-(4,5-Dihydro-1*H*-imidazol-2-yl)aniline (40 mg, 0.25 mmol) was dissolved in 1.5 mL of glacial acetic acid before being added to the acid chloride. The solution was sonicated to mix before being allowed to react overnight at room temperature. The solvent was removed, and crude product was purified on a 50 g C18 reversed-phase column (acetonitrile/water). The product was obtained as a TFA salt (15 mg, 12% yield). ^1H NMR (400 MHz, DMSO- d_6) δ 10.93 (s, 1H), 10.37 (s, 2H), 8.62 (s, 1H), 8.35 (d, $J = 2.0$ Hz, 1H), 8.08 (m, 5H), 7.96 (d, $J = 8.8$ Hz, 2H), 7.78 (dd, $J = 8.8, 2.0$ Hz, 1H), 4.01 (s, 4H). ^{13}C NMR (400 MHz, DMSO- d_6) δ 166.09, 164.44, 144.79, 135.58, 132.22, 131.23, 130.59, 130.11, 129.74, 129.56, 128.46, 127.51, 125.61, 121.58, 119.92, 116.60, 44.32. HRMS: m/z calcd for $\text{C}_{20}\text{H}_{16}\text{BrN}_3\text{O}$ $[\text{M} + \text{H}]^+$ 394.0557; found $[\text{M} + \text{H}]^+$ 394.0553.

4-(Benzylcarbamoyl)benzoyl Chloride (**18**). To a solution of terephthalic acid (300 mg, 1.8 mmol) in 5 mL of dichloromethane and 1.0 mL of DMF was added sequentially diisopropylethylamine (0.95 mL, 5.4 mmol) and benzylamine (0.11 mL, 1.08 mmol). This mixture was stirred together at rt for 30 min followed by addition of TBUTU (415 mg, 1.26 mmol). The mixture was stirred at rt overnight. By LC-MS, the desired monoaddition product was the major one. The reaction was stopped by addition of water, resulting in a small of a white precipitate to form. This was filtered off and determined to be the bis-amide product. The resulting biphasic mixture was separated, and the aqueous layer was extracted with dichloromethane (4 \times). The organics were combined, dried, and concentrated in vacuo to give a thick oil. Addition of a few drops of water to this oil resulted in a thick precipitate forming that was filtered and washed successively with water and diethyl ether (2 \times) to give a resulting white solid of 95% purity which was carried on in the next step. ^1H NMR (400 MHz, DMSO- d_6) δ 9.21 (t, $J = 6$ Hz, 1H), 8.03–7.85 (m, 4H), 7.41–7.32 (m, 4H), 7.24–7.20 (m, 1H), 4.49 (d, $J = 6$ Hz, 2H).

The resulting acid (65 mg, 0.25 mmol) from above was added to a reaction vial with a stir bar and fitted with a Teflon cap and dissolved in 1.5 mL of dichloromethane. The reaction was then cooled to 0 $^{\circ}\text{C}$, and a catalytic amount of DMF was added to the reaction. To this solution was added a 2.0 M solution of oxalyl chloride (0.14 mL, 0.28 mmol) in dichloromethane. The resulting mixture was stirred for 10 min at 0 $^{\circ}\text{C}$ and then allowed to warm to rt. After stirring for 1 h at rt, the reaction was concentrated to dryness under vacuum. The resulting residue was then used as is in the next step.

Methyl 2-Benzyl-1-oxoisindoline-5-carboxylate (**20**). To a screwtop vial fitted with a Teflon cap was added methyl 1-oxoisindoline-5-carboxylate (100 mg, 0.52 mmol). To this was added cesium carbonate (252 mg, 0.78 mmol), and the resulting mixture was slurried in 4 mL of acetonitrile. Benzyl bromide (0.08 mL, 0.68 mmol) was added to the reaction, which was subsequently heated to 75 $^{\circ}\text{C}$ and allowed to stir at this temperature overnight. Additional cesium carbonate (100 mg, 0.3 mmol) and benzyl bromide (0.03 mL, 0.25 mmol) and the reaction and heating again overnight led to complete consumption of starting material. The reaction was allowed to cool to rt, and the solvent was removed by passing a gentle stream of air over the top of the vial. To the resulting residue was added water and dichloromethane. The layers were separated, and the aqueous layer was extracted with dichloromethane (4 \times). The organics were

combined, dried over magnesium sulfate, and concentrated in vacuo. The crude product was purified by flash chromatography using a 40 g Teledyne Isco Redisepp column. Elution with hexanes–EtOAc (5:1 → 2:1) gave 70 mg (48%) of the desired product as a white solid. ¹H NMR (400 MHz, DMSO-*d*₆) δ 8.16 (d, *J* = 8.0 Hz, 1H), 8.07 (s, 1H), 7.95 (d, *J* = 8.0 Hz, 1H), 7.40–7.30 (m, 5H), 4.83 (s, 2H), 4.32 (s, 2H), 3.96 (s, 3H).

Molecular Modeling. Docked poses of **1** and selected analogues were obtained using a procedure described previously²⁰ and summarized here. Marvin Calculator Plugins³³ were used to assign the most likely protonation and tautomerization state for each compound. A full-length model of monomeric AcrA was generated with an X-ray structure of truncated AcrA lacking 21 residues at the N-terminus and the entire membrane-proximal domain (PDB entry 2F1M).¹³ An X-ray structure of CusB from *E. coli*³⁴ was used as the template for the MP domain. After a brief molecular dynamics (MD) simulation of the model in water, the resulting MD snapshots were clustered to generate a diverse ensemble of conformations. Ensemble docking³⁵ was then performed on each protein conformation with VinaMPI³⁶ to generate and rank ligand binding poses. Selected 2D and 3D molecular descriptors were calculated with the program MOE.³⁷

Biology. *E. coli* WT-pore and ΔTolC-pore strains are derivatives of BW 25113 and GD102.²¹ Plasmid pEZ11 expressing a soluble AcrA^{His} variant under the IPTG-inducible T7-promoter was used for purification of AcrA.³⁸ MICs were analyzed using a 2-fold broth dilution method.³⁹ For the checkerboard assay, an antibiotic and a test compound were serially diluted into 96-well plates as described previously.⁴⁰ SPR experiments were carried out with the purified AcrA immobilized onto a CM5 chip (Biacore).^{20,22} The SPR assay was validated using both negative and positive controls, as described previously.²⁰ The HT uptake assay was performed in a temperature-controlled microplate reader (Tecan Spark 10M) equipped with a sample injector, in fluorescence mode. Data were fitted to extract initial rates, as described previously.²⁰ The effect of compounds on the transmembrane potential was analyzed using DiSC3(5), as described previously.⁴¹ The ionophore valinomycin was used as a positive control. This ionophore, which is usually inactive against Gram-negative bacteria, depolarizes the inner membrane of *E. coli* WT-pore cells because it can reach into the periplasm through the large nonspecific pore present in the outer membrane of these cells.

To measure transmembrane potential, exponentially grown and induced WT-pore cells were collected, washed, and resuspended to the final OD₆₀₀ of 0.2 in a buffered glucose solution supplemented with either valinomycin or indicated EPIs in final concentration 10 μM. Then 1% DMSO was added as a negative control. Cells were added to the same buffer solution containing 1 μM of the voltage-sensitive probe DiSC3(5). Upon addition of cells, the DiSC3(5) fluorescence quenched due to the presence of transmembrane potential.

To test for cytotoxicity, the Promega Cell Titer Glo luminescent cell viability assay was used according to manufacturer's protocol. HEK293 cells (ATCC CRL-1573) were plated in 96-well white plates with clear, tissue culture-treated flat bottoms (Corning 3903) at 20000 cells per well in 75 μL of DMEM media (Gibco) with 5% FBS (Gemini Biosystems) and L-glutamine (Corning) added. Cells were incubated at 37 °C overnight in the presence of 5% CO₂. The next day, compounds of interest were serially diluted and added to the cells to make a total volume of 100 μL per well, with DMSO used as a negative control. Cells were again incubated overnight in 37 °C with 5% CO₂. The following day, ATP standards were added to corresponding wells and luminescent substrate was added to all wells and incubated for 10 min at room temperature. Luminescence was measured on a Biotek Neo plate reader according to manufacturer's protocol. Data was analyzed using Graphpad Prism Software using standard LD₅₀ nonlinear regression analysis.

■ ASSOCIATED CONTENT

■ Supporting Information

The Supporting Information is available free of charge on the ACS Publications website at DOI: 10.1021/acs.jmedchem.7b00453.

Figures depicting additional docking poses for **1**, **4a–e**, and **11**, molecular descriptor analysis of all new compounds, detailed characterization of compounds **1**, **17h**, **17o**, and **17q**, characterization of intermediates **9a**, **11**, and **16**, and LC-MS traces for all reported compounds (PDF)

Molecular formula strings (CSV)

■ AUTHOR INFORMATION

Corresponding Author

*Phone: 1-314-977-6427. E-mail: walkerjk@slu.edu.

ORCID

Jerry M. Parks: 0000-0002-3103-9333

Valentin V. Rybenkov: 0000-0002-5300-4369

John K. Walker: 0000-0002-8683-0026

Notes

The authors declare no competing financial interest.

■ ACKNOWLEDGMENTS

The University of Saint Louis School of Medicine and the National Institutes of Health AI052293 (H.I.Z.) supported this work. We thank the Drug Synthesis and Chemistry Branch, Developmental Therapeutics Program, NCI, USA, for providing us with plated and vial samples. We gratefully acknowledge Dr. Stacy Arnett and the Center for World Health & Medicine for performing high-resolution mass spectrometry experiments. We acknowledge Dr. Kristine Griffett for performing cytotoxicity measurements on compounds **17h** and **17o**. We also acknowledge Miss Ashley Anderson and the NMR facility in the Saint Louis University Department of Chemistry for acquiring ¹H and ¹³C NMR spectra. We thank Mr. David Wolloscheck at the University of Oklahoma for help with fitting the kinetic data and Sarah J. Cooper for calculating molecular descriptors.

■ ABBREVIATIONS USED

DCM, dichloromethane; DMAC, dimethylacetamide; DMF, dimethylformamide; DMSO, dimethyl sulfoxide; EPI, efflux pump inhibitor; EtOAc, ethyl acetate; HOAc, glacial acetic acid; MPC, minimum potentiation concentration; MW, molecular weight; NCI, National Cancer Institute; NIH, National Institutes of Health; OM, outer membrane; SPR, surface plasmon resonance; TBTU, O-(benzotriazol-1-yl)-N,N,N',N'-tetramethyluronium tetrafluoroborate; TFA, trifluoroacetic acid; WT, wild-type

■ REFERENCES

- (1) Page, M. GP; Heim, J. Prospects for the next anti-*Pseudomonas* drug. *Curr. Opin. Pharmacol.* **2009**, 9, 558–565.
- (2) Dorotkiewicz-Jach, A.; Augustyniak, D.; Olszak, T.; Drulis-Kawa, Z. Modern therapeutic approaches against *Pseudomonas aeruginosa*. *Curr. Med. Chem.* **2015**, 22, 1642–1664.
- (3) Delcour, A. Outer membrane permeability and antibiotic resistance. *Biochim. Biophys. Acta, Proteins Proteomics* **2009**, 1794, 808–816.

- (4) Poole, K.; Srikumar, R. Multidrug Efflux in *Pseudomonas aeruginosa*: Components, mechanisms and Clinical Significance. *Curr. Top. Med. Chem.* **2001**, *1*, 59–71.
- (5) Nikaido, H.; Pages, J.-M. Broad-specificity efflux pumps and their role in multidrug resistance of Gram-negative bacteria. *FEMS Microbiol. Rev.* **2012**, *36*, 340–363.
- (6) Mazzariol, A.; Zuliani, J.; Cornaglia, G.; Rossolini, G. M.; Fontana, R. AcrAB efflux system: expression and contribution to fluoroquinolone resistance in *Klebsiella* spp. *Antimicrob. Agents Chemother.* **2002**, *46*, 3984–3986.
- (7) Nakashima, R.; Sakurai, K.; Yamasaki, S.; Hayashi, K.; Nagata, C.; Hoshino, K.; Onodera, Y.; Nishino, K.; Yamaguchi, A. Structural basis for the inhibition of bacterial multidrug exporters. *Nature* **2013**, *500*, 102–106.
- (8) Opperman, T. J.; Nguyen, S. T. Recent advances toward a molecular mechanism of efflux pump inhibition. *Front. Microbiol.* **2015**, *6*, 421.
- (9) Jamshidi, S.; Sutton, J. M.; Rahman, K. M. An overview of bacterial efflux pumps and computational approaches to study efflux pump inhibitors. *Future Med. Chem.* **2016**, *8*, 195–215.
- (10) Nikaido, H.; Zgurskaya, H. I. AcrAB and related multidrug efflux pumps of *Escherichia coli*. *J. Mol. Microbiol. Biotechnol.* **2001**, *3*, 215–218.
- (11) Krishnamoorthy, G.; Tikhonova, E. B.; Dhamdhare, G.; Zgurskaya, H. I. On the role of TolC in multidrug efflux: the function and assembly of AcrAB-TolC tolerate significant depletion of intracellular TolC protein. *Mol. Microbiol.* **2013**, *87*, 982–997.
- (12) Du, D.; Wang, Z.; James, J. R.; Voss, J. E.; Klimont, E.; Ohene-Agyei, T.; Venter, H.; Chiu, W.; Luisi, B. F. Structure of the AcrAB-TolC multidrug efflux pump. *Nature* **2014**, *509*, 512–515.
- (13) Mikolosko, J.; Bobyk, K.; Zgurskaya, H. I.; Ghosh, P. Conformational flexibility in the multidrug efflux system protein AcrA. *Structure* **2006**, *14*, 577–587.
- (14) Jeong, H.; Kim, J. S.; Song, S.; Shigematsu, H.; Yokoyama, T.; Hyun, J.; Ha, N. C. Pseudoatomic structure of the tripartite multidrug efflux pump AcrAB-TolC reveals the intermeshing cogwheel-like interaction between AcrA and TolC. *Structure* **2016**, *24*, 272–276.
- (15) Vargiu, A. V.; Nikaido, H. Multidrug binding properties of the AcrB efflux pump characterized by molecular dynamics simulations. *Proc. Natl. Acad. Sci. U. S. A.* **2012**, *109*, 20637–20642.
- (16) Lu, W.; Zhong, M.; Chai, Q.; Wang, Z.; Yu, L.; Wei, Y. Functional relevance of AcrB trimerization in pump assembly and substrate binding. *PLoS One* **2014**, *9*, e89143.
- (17) Blair, J. M.; Bavro, V. N.; Ricci, V.; Modi, N.; Cacciottolo, P.; Kleinekathöfer, U.; Ruggerone, P.; Vargiu, A. V.; Baylay, A. J.; Smith, H. E.; Brandon, Y.; Galloway, D.; Piddock, L. J. AcrB drug-binding pocket substitution confers clinically relevant resistance and altered substrate specificity. *Proc. Natl. Acad. Sci. U. S. A.* **2015**, *112*, 3511–3516.
- (18) Bohnert, J. A.; Schuster, S.; Kern, W. V.; Karcz, T.; Olejars, A.; Kaczor, A.; Handzlik, J.; Kiec-Kononowicz, K. Novel piperazine arylideneimidazolones inhibit the AcrAB-TolC pump in *Escherichia coli* and simultaneously act as fluorescent probes in a combined real-time influx and efflux assay. *Antimicrob. Agents Chemother.* **2016**, *60*, 1974–1983.
- (19) Sjuts, H.; Vargiu, A. V.; Kwasny, S. M.; Nguyen, S. T.; Kim, H.-S.; Ding, X.; Ornik, A. R.; Ruggerone, P.; Bowlin, T. L.; Nikaido, H.; Pos, K. M.; Opperman, T. J. Molecular basis for the inhibition of AcrB multidrug efflux pump by novel and powerful pyranopyridine derivatives. *Proc. Natl. Acad. Sci. U. S. A.* **2016**, *113*, 3509–3514.
- (20) Abdali, N.; Parks, J. M.; Haynes, K. M.; Chaney, J. L.; Green, A. T.; Wolloscheck, D.; Walker, J. K.; Rybenkov, V. V.; Baudry, J.; Smith, J. C.; Zgurskaya, H. I. Reviving antibiotics: efflux pump inhibitors that interact with AcrA, a membrane fusion protein of the AcrAB-TolC multidrug efflux pump. *ACS Infect. Dis.* **2017**, *3*, 89–98.
- (21) Krishnamoorthy, G.; Wolloscheck, D.; Weeks, J. W.; Croft, C.; Rybenkov, V. V.; Zgurskaya, H. I. Breaking the permeability barrier of *Escherichia coli* by controlled hyperporination of the outer membrane. *Antimicrob. Agents Chemother.* **2016**, *60*, 7372–7381.
- (22) Tikhonova, E. B.; Dastidar, V.; Rybenkov, V. V.; Zgurskaya, H. I. Kinetic control of TolC recruitment by multidrug efflux complexes. *Proc. Natl. Acad. Sci. U. S. A.* **2009**, *106*, 16416–16421.
- (23) Wander, A. G. Polybasic compounds and processes for their production. GB patent 1007334, 1965.
- (24) Pine, M. J.; Harzewski, E.; Wissler, F. C. Action of Phthalanilide drugs on *Escherichia coli*. *Cancer Res.* **1963**, *23*, 932–937.
- (25) Yesair, D. W.; Kohner, F. A.; Rogers, W. L.; Baronowsky, P. E.; Kensler, C. J. Relationship of the phthalanilide-lipid complexes to uptake and retention of 2-chloro-4',4''-di(2-imidazolin-2-yl)-terephthalanilide (NSC 60339) by sensitive and resistant p388 leukemia cells. *Cancer Res.* **1966**, *26*, 202–207.
- (26) Coldham, N. G.; Webber, M.; Woodward, M. J.; Piddock, L. J. V. A 96-well plate fluorescence assay for assessment of cellular permeability and active efflux in *Salmonella enterica* serovar Typhimurium and *Escherichia coli*. *J. Antimicrob. Chemother.* **2010**, *65*, 1655–1663.
- (27) Sun, M.; Wei, H.-T.; Li, D.; Zheng, Y.-G.; Cai, J.; Ji, M. Mild and efficient one-pot synthesis of 2-imidazolines from nitriles using sodium hydrosulfide as catalyst. *Synth. Commun.* **2008**, *38*, 3151–3158.
- (28) Hagmann, W. K. Substituted aminoquinolines as modulators of chemokine receptor activity. WO 98/27815, 1998.
- (29) Dong, Y.; Wang, X.; Cal, M.; Kaiser, M.; Vennerstrom, J. L. Activity of diimidazoline amides against African trypanosomiasis. *Bioorg. Med. Chem. Lett.* **2014**, *24*, 944–948.
- (30) Chollet, R.; Chevalier, J.; Bryskier, A.; Pages, J.-M. The AcrAB-TolC pump is involved in macrolide resistance but not in telithromycin efflux in *Enterobacter aerogenes* and *Escherichia coli*. *Antimicrob. Agents Chemother.* **2004**, *48*, 3621.
- (31) Richter, M. F.; Drown, B. S.; Riley, A. P.; Garcia, A.; Shirai, T.; Svec, R. L.; Hergenrother, P. J. Predictive compound accumulation rules yield a broad-spectrum antibiotic. *Nature* **2017**, *545*, 299–304.
- (32) Baell, J. B.; Holloway, G. A New substructure filters for removal of pan assay interference compounds (PAINS) from screening libraries and for their exclusion in bioassays. *J. Med. Chem.* **2010**, *53*, 2719–2740.
- (33) Calculator Plugins were used for structure property prediction and calculation : Marvin 17.9.0, ChemAxon: Cambridge, MA, 2017; <http://www.chemaxon.com>.
- (34) Su, C.-C.; Long, F.; Zimmermann, M. T.; Rajashankar, K. R.; Jernigan, R. L.; Yu, E. W. Crystal structure of the CusBA heavy-metal efflux complex of *Escherichia coli*. *Nature* **2011**, *470*, 558–562.
- (35) Ellingson, S. R.; Miao, Y.; Baudry, J.; Smith, J. C. Multi-conformer ensemble docking to difficult protein targets. *J. Phys. Chem. B* **2015**, *119*, 1026–1034.
- (36) Ellingson, S. R.; Smith, J. C.; Baudry, J. VinaMPI: facilitating multiple receptor high-throughput virtual docking on high-performance computers. *J. Comput. Chem.* **2013**, *34*, 2212–2221.
- (37) Molecular Operating Environment (MOE); Chemical Computing Group ULC: 1010 Sherbrooke St. West, Suite #910, Montreal, Quebec H3A 2R7, Canada, 2015.
- (38) Zgurskaya, H. I.; Nikaido, H. AcrA is a highly asymmetric protein capable of spanning the periplasm. *J. Mol. Biol.* **1999**, *285*, 409–420.
- (39) Tikhonova, E. B.; Wang, Q.; Zgurskaya, H. I. Chimeric analysis of the multicomponent multidrug efflux transporters from Gram-negative bacteria. *J. Bacteriol.* **2002**, *184*, 6499–6507.
- (40) Lomovskaya, O.; Warren, M. S.; Lee, A.; Galazzo, J.; Fronko, R.; Lee, M.; Blais, J.; Cho, D.; Chamberland, S.; Renau, T.; leger, R.; Hecker, S.; Watkins, W.; Hoshino, K.; Ishida, H.; Lee, V. J. Identification and characterization of inhibitors of multidrug resistance efflux pumps in *Pseudomonas aeruginosa*: novel agents for combination therapy. *Antimicrob. Agents Chemother.* **2001**, *45*, 105–116.
- (41) Farha, M. A.; Verschoor, C. P.; Bowdish, D.; Brown, E. D. Collapsing the Proton Motive Force to Identify Synergistic Combinations against *Staphylococcus aureus*. *Chem. Biol.* **2013**, *20*, 1168–1178.